IEEE Access
Multidisciplinary ⋮ Rapid Review ⋮ Open Access Journal

Received April 7, 2022, accepted April 25, 2022, date of publication May 2, 2022, date of current version May 6, 2022.

Digital Object Identifier 10.1109/ACCESS.2022.3171580

PI Observer-Based Fault-Tolerant Tracking Controller for Automobile Active Suspensions

JIBO LUO, HUI PANG, (Member, IEEE), MINGXIANG WANG, AND RUI YAO
School of Mechanical and Precision Instrument Engineering, Xi'an University of Technology, Xi'an 710048, China

Corresponding author: Hui Pang (huipang@163.com)

This work was supported by the National Natural Science Foundation of China under Grant 51675423.

ABSTRACT The objective of this paper is to retain the desirable dynamics performances and improve ride quality for active suspensions with the actuator faults and unknown road disturbances. To that end, a novel proportional-integral observer (PIO)-based fault-tolerant tracking controller (FTTC) design is proposed for automobile active suspensions (ASSs) encountered with actuator faults and parameter uncertainties. First, the Takagi-Sugeno (T-S) fuzzy model approach is adopted to establish T-S representation of the faulty ASSs by describing vehicle dynamics system as the weighed summation of a common linear system. Afterwards, a nominal robust H_∞ output feedback controller is developed to enhance the suspension performances under fault-free mode, whose output response indicators are taken as the prescribed reference trajectories. Then, a PIO-based fault estimator is designed to predict both the system states and the unmeasurable actuator faults, synchronously. On basis of this designed observer, the expected PIO-FTTC is synthesized to track the prescribed reference trajectories, and further to make up for the system performance deteriorations aroused by the actuator faults. Finally, a simulative investigation demonstrates the effectiveness and feasibility of the proposed PIO-FTTC compared to existing control approach.

INDEX TERMS Automobile active suspensions, T-S fuzzy model approach, fault-tolerant tracking controller, proportional-integral observer.

I. INTRODUCTION

It is well acknowledged that automobile active suspensions (ASSs) have great potentialities to attain a well trade-off between the hardware cost and control performance in design process of the chassis system [1]. At present, a number of control schemes dedicated to vehicle ASS have been developed, such as sliding-mode control [2], adaptive backstepping control [3], [4], robust control [5] and fuzzy logic control [6], [7], along with neural-network control [8]. Nevertheless, the early scholars have conducted their studies and presented some control strategies for ASSs supposed that all the components and actuators work under normal (fault-free) operations, which is obviously inconsistent with the actual working situation of active suspension system. Because in reality, suspension system components will inevitably fail, which will bring challenges to the control of active suspension system.

In fact, faults or failures may be commonly encountered in actuators, sensors or system itself no matter in aerospace devices and spacecraft [9]–[11], or in vehicle active suspensions [12]–[18], this could cause severe performance degradation and instability for the controlled systems, thus it is necessary to solve this problem by design an appropriate fault-tolerant controller (FTC). For instances, in the work of [9], an indirect robust adaptive FTC was proposed to realize the efficient attitude tracking control of a spacecraft. In [10], a type of adaptive fault-tolerant tracking controller (FTTC) was presented to expect to reduce the fault effects on the aircraft control plant in terms of online estimation information of actuator fault, yet a suitable fault detection and isolation principle was lacked. In [11], a uniform adaptive FTTC scheme was proposed trough real-time online estimation of the underlying actuator faults, wherein a control unit was adopted to eliminate and/or weaken the negative effect of actuator faults.

When developing the control algorithm for the fault active suspension system, it is necessary to ensure that the control algorithm can compensate the fault, so as to reduce the influence of actuator fault on the performance of the suspension system. Compared with the active suspension system without actuator faults, the performance of the active

The associate editor coordinating the review of this manuscript and approving it for publication was Wenbing Zhao.

suspension system under fault-tolerant control algorithm has little change. In the work of [12], the FTTC design was proposed to enhance ride comfort and handling stability of vehicle described by a Takagi-Sugeno (T-S) fuzzy model with immeasurable premise variables in continuous time domain. In [13], A novel adaptive sliding fault tolerant controller, which does depend on accurate models, was designed to stabilize the active suspension systems and thus to improve the ride comfort, without utilizing the bounds of actuator faults and parameter uncertainties. In [14], a method for estimating road-shore angles and faults of linear vehicle models based on unknown input proportional integral (PI) observer was proposed. The goal is to estimate simultaneously, the states, the road bank angle and the faults of the system in the presence of disturbance input. In [15], a fault-tolerant controller was proposed based on sliding mode observer for a class of active suspension systems with parameter uncertainties and sensor faults. In [16], a novel adaptive sliding-based FTC was implemented with the purpose of stabilizing the ASSs and to improve ride quality of vehicle, yet the negative effects of actuator faults and parameter uncertainties were usually ignored. In [17], an adaptive FTC method was proposed based on the uncertain dynamics model of the vehicle, and a compensation controller was derived for nonlinear ASS. Moreover, in the work of [18], a fuzzy proportional-integral (PI) controller was proposed using genetic algorithm to improve the ride quality of passengers of ASSs. In [19], a proportional integral sliding mode control scheme was designed for a quarter of the vehicle active suspension system, and a robust PI observer (PIO) for fault detection, isolation and amplitude estimation of uncertain linear time-invariant systems was proposed to estimate the control system state and actuator faults of a certain type of vehicle suspension [20]. These control techniques inspire us to develop the desired FTTC along this direction.

On the other hand, one major difficulty of the FTC controller for the ASS is that there often exist the parameter uncertainties resulted from the variations of payloads or passenger numbers, which are usually ignored and may impose some negative effects on the controlled active suspensions [21]. To address such problem for the FTC design in vehicle ASS, T-S fuzzy model (TSFM) approach is employed to depict the parametric uncertainties of ASSs by using the fuzzy sets and IF-THEN rules [22], [23]. For example, in the work of [24], the adaptive SMC was presented for the ASS using TSFM method, wherein the uncertainties of vehicle-body mass, the unknown actuator's nonlinearities, as well as the suspension deflection performances were tackled simultaneously. In [25], the optimization H∞ nonparallel distribution compensation control issue for nonlinear systems under Takagi-Sugeno (T-S) fuzzy framework was studied. In [26], TSFM approach was also utilized to denote the variations of vehicle-body mass, thus a robust H_∞ control scheme was designed to guarantee the desired performances of uncertain ASS with sensor failures. The authors in [27] have rendered the nonlinear semi-active suspension model into the linear subsystems connected by the fuzzy-membership functions via T-S approach, and then proposed a fuzzy observer-based control design method. It has to be admitted that those studies provide us great inspiration for dealing with the actuator fault constrained ASS. Additionally, in most of the previous literatures, although many researchers have investigated the related FTC method for vehicle ASS subjected to actuator and/or sensor faults, parameter uncertainties that generally exist in the practical suspension systems are usually ignored, and the system states and actuator faults are directly fed back to the corresponding controller or are estimated separately when developing the corresponding FTC controller, which may bring about some difficulties in the controller design.

To that end, this paper is focused on proposing a composite PIO-based FTTC scheme for the uncertain ASS with the unknown actuator faults using TSFM approach. Compared with the previous related studies in [17]–[19], the main contributions of this study can be summarized as follows:

(1) T-S fuzzy method is used to reconstruct the active suspension system with parameter uncertainty under the influence of disturbance and fault, which increases the accuracy of the fault suspension model.

(2) In this paper, a compound fault-tolerant tracking control method based on PI observer (PIO-FTTC) is designed by integrating the characteristics of both PI observer and FTC fault-tolerant tracking controller with the classical robust output feedback control (ROFC). A new idea is provided for optimizing the fault suspension control system and properly solving the fault tolerant control problem of active suspension system with parameter uncertainty under the influence of disturbance and fault.

(3) A key difference between this design and the existing reliable control designs is that the proposed controller enables the normal tracking performance of the closed-loop system optimized by the LMI method without any conservatism, and makes the state of the failure mode asymptotically tracked with the state of ASS in the normal mode. This makes sense because the system runs under normal conditions most of the time. The proposed method is based on the online estimation of faults and adds a new control method to the normal control method. It does not need to design a separate fault diagnosis and isolation mechanism (FDI) for the failed system to reduce the impact of faults on the system, which greatly reduces the complexity of the system.

Finally, an illustrative example is provided to display the advantages of our designed FTTC scheme under different running conditions. The control method proposed in this paper is suitable for the mechanical vibration system affected by actuator faults, so as to achieve the purpose of fault compensation control, and then stabilize the system.

The rest of this paper is structured as follows. Section II presents the system model for ASSs with actuator and road disturbances using TSFM approach. In Section III, the design of FTTC scheme is described in detail. Section IV provides

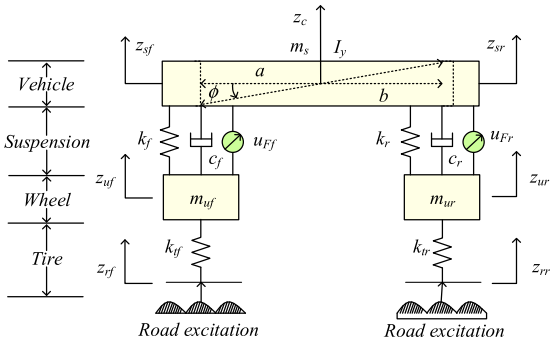

FIGURE 1. The schematic diagram of half ASS model.

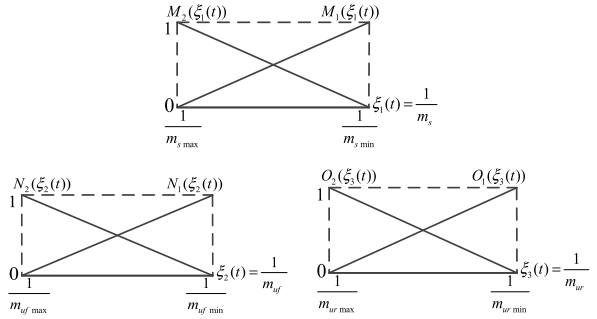

FIGURE 2. Membership functions.

the simulation investigations of the developed FTTC scheme. Finally, the study results are drawn in Section V.

Notations: The symbol $*$ stands for the transposed element in the symmetric positions of a matrix, $diag\{\Theta_1, \ldots, \Theta_r\}$ stands for a block diagonal matrix which diagonal entries are defined by $\Theta_1, \cdots, \Theta_r$. I denote identity matrix with appropriate dimension.

II. SYSTEM MODELING AND PROBLEM STATEMENT

A. T-S REPRESENTATION FOR UNCERTAIN ACTIVE SUSPENSIONS

As shown in Fig. 1, a half ASS model that has been extensively employed in suspension research [4], [28] is used to describe vehicle motions and dynamics behaviors, in which a, b represent the distances from the front- and rear- (FR) axles to the center of gravity (COG) in vehicle center of mass, respectively; m_s and I_y represent the sprung mass and the pitch moment of inertia at the COG, respectively; z_c, ϕ represent the vertical and pitch angular displacements at the COG, respectively; m_{uf}, m_{ur} denote the unsprung mass of the FR suspensions, respectively; c_f, c_r are the damping coefficients of the FR suspensions, respectively; k_f, k_r are the stiffness coefficients of the FR suspensions, respectively; z_{uf}, z_{ur} stand for the vertical displacements of the FR unsprung mass, respectively; k_{tf}, k_{tr} stand for the tire stiffness coefficients of the FR tires, respectively; z_{rf}, z_{rr} stand for the road disturbances at the FR wheels, respectively; u_{Ff}, u_{Fr} denote the control forces generated by the FR actuator, respectively. The dynamic characteristics of the actuator itself are ignored in this paper.

In terms of Newton's second law, the dynamics equations of ASS model are established as

$$\begin{cases} m_s\ddot{z}_c(t) = F_1(t) + F_2(t) \\ I_y\ddot{\phi}(t) = bF_2(t) - aF_1(t) \\ m_{uf}\ddot{z}_{uf}(t) = -F_{tf}(t) - F_1(t) \\ m_{ur}\ddot{z}_{ur}(t) = -F_{tr}(t) - F_2(t) \end{cases} \tag{1}$$

where

$$\begin{cases} F_1(t) = k_f\Delta y_f(t) + c_f\left(\dot{z}_{sf}(t) - \dot{z}_{uf}(t)\right) + u_{Ff}(t) \\ F_2(t) = k_r\Delta y_r(t) + c_r\left(\dot{z}_{sr}(t) - \dot{z}_{ur}(t)\right) + u_{Fr}(t) \end{cases} \tag{2}$$

$$\begin{cases} F_{tf}(t) = k_{tf}(z_{uf}(t) - z_{rf}(t)) \\ F_{tr}(t) = k_{tr}(z_{ur}(t) - z_{rr}(t)) \end{cases} \tag{3}$$

wherein $\Delta y_f(t) = z_{sf}(t) - z_{uf}(t)$ is the front suspension deflection, $\Delta y_r(t) = z_{sr}(t) - z_{ur}(t)$ is the deflection at the rear-wheel. Here, the vertical displacements of the FR suspension are denoted by $z_{sf}(t)$ and $z_{sr}(t)$, respectively, which satisfy $z_{sf}(t) = z_c(t) + a\tan\phi(t) \approx z_c(t) + a\phi(t)$ and $z_{sr}(t) = z_c(t) - b\tan\phi(t) \approx z_c(t) - b\phi(t)$ in terms of literature [28] when $\phi(t)$ is set a small value.

Define the state vector as $\boldsymbol{x}(t) = [z_c(t), \dot{z}_c(t), \phi(t), \dot{\phi}(t), z_{uf}(t), z_{ur}(t), \dot{z}_{uf(t)}, \dot{z}_{ur}(t)]^T$, the road disturbance vector as $\boldsymbol{w}(t) = [z_{rf}(t), z_{rr}(t)]^T$, and the control force vector as $\boldsymbol{u}_f(t) = [u_{Ff}(t), u_{Fr}(t)]^T$, moreover, the measurable output vector is chosen as $\boldsymbol{y}(t) = [\dot{z}_c(t), \dot{\phi}(t)]^T$, and the control output vector is defined as $\boldsymbol{z}(t) = [\ddot{z}_c(t), \dot{\phi}(t), z_{sf}(t) - z_{uf}(t), z_{sr}(t) - z_{ur}(t), k_{tf}(z_{uf}(t) - z_{rf}(t)), k_{tr}(z_{ur}(t) - z_{rr}(t)), u_{Ff}(t), u_{Fr}(t)]^T$. Then, based on (1) to (3), the state-space form of this ASS is then written as

$$\begin{cases} \dot{\boldsymbol{x}}(t) = \boldsymbol{A}\boldsymbol{x}(t) + \boldsymbol{B}\boldsymbol{u}_n(t) + \boldsymbol{B}_1\boldsymbol{w}(t) \\ \boldsymbol{y}(t) = \boldsymbol{C}\boldsymbol{x}(t) \\ \boldsymbol{z}(t) = \boldsymbol{C}_1\boldsymbol{x}(t) + \boldsymbol{D}_1\boldsymbol{u}_n(t) + \boldsymbol{E}_1\boldsymbol{w}(t) \end{cases} \tag{4}$$

wherein $\boldsymbol{A}, \boldsymbol{B}, \boldsymbol{B}_1, \boldsymbol{C}, \boldsymbol{D}, \boldsymbol{C}_1, \boldsymbol{D}_1$ and $\boldsymbol{E}_1$ are the corresponding coefficient matrices with an appropriate dimension, see them in APPENDIX A.

Since the passenger numbers and vehicle payloads are usually changed, the variations and uncertainties of m_s, m_{uf} and m_{ur} should be considered, which can be expressed as $m_s \in [m_{s\_\min}, m_{s\_\max}]$, $m_{uf} \in [m_{uf\_\min}, m_{uf\_\max}]$ and $m_{ur} \in [m_{ur\_\min}, m_{ur\_\max}]$, where $m_{j\_\min}$ and $m_{j\_\max}$ denote the lower and upper bounds of m_j $(j = s, u_f, u_r)$. Thus, the TSFM for normal ASS with the parametric uncertainties can be established by defining the following scales [29] as

$$\left.\begin{aligned} m_s^i(t) &= M_1(\xi_1(t))\left(m_{s_{\min}}^i\right) + M_2(\xi_1(t))\left(m_{s_{\max}}^i\right) \\ m_{uf}^i(t) &= N_1(\xi_2(t))\left(m_{uf_{\min}}^i\right) + N_2(\xi_2(t))\left(m_{uf_{\max}}^i\right) \\ m_{ur}^i(t) &= O_1(\xi_3(t))\left(m_{ur_{\min}}^i\right) + O_2(\xi_3(t))\left(m_{ur_{\max}}^i\right) \end{aligned}\right\} \tag{5}$$

where $\xi_1(t) = 1/m_s(t)$, $\xi_2(t) = 1/m_{uf}(t)$, $\xi_3(t) = 1/m_{ur}(t)$, and the mass inverse expression $m_q^I = 1/m_q$ is used to avoid

a large fractions, then we have $m_j^i(t) = 1/m_j(t), m_{j\_\min}^i = 1/m_{j\_\max}, m_{j\_\max}^i = 1/m_{j\_\max}$. In a similar way, the membership functions of $M_1(\xi_1(t))$, $M_2(\xi_1(t))$, $N_1(\xi_2(t))$, $N_2(\xi_2(t))$, $O_1(\xi_3(t))$ and $O_2(\xi_3(t))$ can be expressed by

$$\left.\begin{aligned} M_1(\xi_1(t)) &= \frac{m_s^i(t) - m_{s_{\max}}^i}{m_{s_{\min}}^i - m_{s_{\max}}^i}, \\ M_2(\xi_1(t)) &= \frac{m_{s_{\min}}^i - m_s^i(t)}{m_{s_{\min}}^i - m_{s_{\max}}^i} \\ N_1(\xi_2(t)) &= \frac{m_{uf}^i(t) - m_{uf_{\max}}^i}{m_{uf_{\min}}^i - m_{uf_{\max}}^i}, \\ N_2(\xi_2(t)) &= \frac{m_{uf_{\min}}^i - m_{uf}^i(t)}{m_{uf_{\min}}^i - m_{uf_{\max}}^i} \\ O_1(\xi_3(t)) &= \frac{m_{ur}^i(t) - m_{ur_{\max}}^i}{m_{ur_{\min}}^i - m_{ur_{\max}}^i}, \\ O_2(\xi_3(t)) &= \frac{m_{ur_{\min}}^i - m_{ur}^i(t)}{m_{ur_{\min}}^i - m_{ur_{\max}}^i} \end{aligned}\right\} \tag{6}$$

It is noted that $M_1(\xi_1(t)) + M_2(\xi_1(t)) = 1$, $N_1(\xi_2(t)) + N_2(\xi_2(t)) = 1$, $O_1(\xi_3(t)) + O_2(\xi_3(t)) = 1$.

The membership function can be expressed as Fig. 2.

Thus, the TSFM of ASS considering the parameter uncertainties is described in the following:

Model Rule *i*: IF $\xi_1(t)$ is $M_r(\xi_1(t))$, $\xi_2(t)$ is $N_j(\xi_2(t))$ and $\xi_3(t)$ is $O_l(\xi_3(t))$,

THEN

$$\begin{aligned} \dot{\boldsymbol{x}}(t) &= \boldsymbol{A}_i\boldsymbol{x}(t) + \boldsymbol{B}_i\boldsymbol{u}_n(t) + \boldsymbol{B}_{1i}\boldsymbol{w}(t) \\ \boldsymbol{y}(t) &= \boldsymbol{C}_i\boldsymbol{x}(t) \\ \boldsymbol{z}(t) &= \boldsymbol{C}_{1i}\boldsymbol{x}(t) + \boldsymbol{D}_{1i}\boldsymbol{u}_n(t) + \boldsymbol{E}_{1i}\boldsymbol{w}(t) \end{aligned} \tag{7}$$

wherein $r = (1, 2)$; $j = (1, 2)$; $l = (1, 2)$; $i = (1, 2, 3, 4, 5, 6, 7, 8)$.

For the related coefficient matrices in (7), $\boldsymbol{A}_i$, $\boldsymbol{B}_i$, $\boldsymbol{B}_{1i}$, $\boldsymbol{C}_i$, $\boldsymbol{D}_i$, $\boldsymbol{C}_{1i}$, $\boldsymbol{D}_{1i}$ and $\boldsymbol{E}_{1i}$ can be obtained by replacing m_j in $\boldsymbol{A}$, $\boldsymbol{B}$, $\boldsymbol{B}_1$, $\boldsymbol{C}$, $\boldsymbol{D}$, $\boldsymbol{C}_1$, $\boldsymbol{D}_1$ and $\boldsymbol{E}_1$ with $m_{j\_\min}$ (or $m_{j\_\max}$), respectively.

Thus, the state-space form of (7) can be inferred using T-S fuzzy approach as follows.

$$\begin{cases} \dot{\boldsymbol{x}}(t) = \sum_{i=1}^{8} h_i(\xi(t)) \begin{pmatrix} \boldsymbol{A}_i\boldsymbol{x}(t) + \boldsymbol{B}_i\boldsymbol{u}_n(t) \\ +\boldsymbol{B}_{1i}\boldsymbol{w}(t) \end{pmatrix} \\ \boldsymbol{y}(t) = \sum_{i=1}^{8} h_i(\xi(t)) (\boldsymbol{C}_i\boldsymbol{x}(t)) \\ \boldsymbol{z}(t) = \sum_{i=1}^{8} h_i(\xi(t)) \begin{pmatrix} \boldsymbol{C}_{1i}\boldsymbol{x}(t) + \boldsymbol{D}_{1i}\boldsymbol{u}_n(t) \\ +\boldsymbol{E}_{1i}\boldsymbol{w}(t) \end{pmatrix} \end{cases} \tag{8}$$

where

$$\begin{aligned} h_1(\xi(t)) &= M_1(\xi_1(t)) \times N_1(\xi_2(t)) \times O_1(\xi_3(t)), \\ h_2(\xi(t)) &= M_1(\xi_1(t)) \times N_2(\xi_2(t)) \times O_1(\xi_3(t)), \\ h_3(\xi(t)) &= M_2(\xi_1(t)) \times N_1(\xi_2(t)) \times O_1(\xi_3(t)), \\ h_4(\xi(t)) &= M_2(\xi_1(t)) \times N_2(\xi_2(t)) \times O_1(\xi_3(t)), \end{aligned}$$

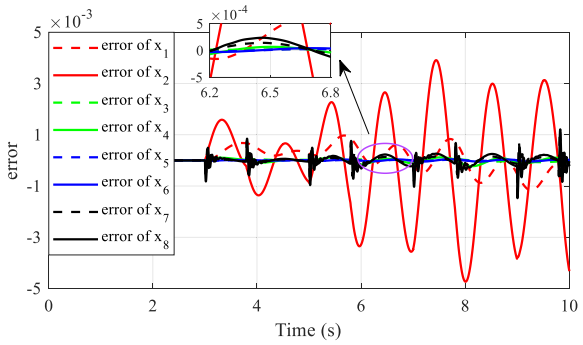

FIGURE 3. The error curve of T-S fuzzy system approximating the ASS.

$$\begin{aligned} h_5(\xi(t)) &= M_2(\xi_1(t)) \times N_2(\xi_2(t)) \times O_2(\xi_3(t)), \\ h_6(\xi(t)) &= M_2(\xi_1(t)) \times N_1(\xi_2(t)) \times O_2(\xi_3(t)), \\ h_7(\xi(t)) &= M_1(\xi_1(t)) \times N_2(\xi_2(t)) \times O_2(\xi_3(t)), \\ h_8(\xi(t)) &= M_1(\xi_1(t)) \times N_1(\xi_2(t)) \times O_2(\xi_3(t)). \end{aligned}$$

Besides, the fuzzy weighting function $h_i(\xi(t))$ should satisfy $h_i(\xi(t)) \geq 0$, $\sum_{i=1}^{8} h_i(\xi(t)) = 1$. For the sake of simplicity, h_i is usually employed to denote $h_i(\xi(t))$.

Remark 1: Herein, m_s, m_{uf} and m_{ur} are considered as a uncertain variables with satisfying $m_s \in [m_{s\_\min}, m_{s\_\max}]$, $m_{uf} \in [m_{uf\_\min}, m_{uf\_\max}]$, $m_{ur} \in [m_{ur\_\min}, m_{ur\_\max}]$, respectively. Besides, the fuzzy weighting function h_i rely on $m_s(t)$, $m_{uf}(t)$ and $m_{ur}(t)$.

B. FAULTY DYNAMICS MODEL OF ACTIVE SUSPENSION SYSTEM

Usually, the actuator faults or failures can be encountered in vehicle ASS, thus the partial fault on the controller design should be considered. Moreover, the actuator faults are added to T-S model of the ASS in order to involve the different types of actuator faults in the subsequent FTTC controller design.

Accordingly, T-S representation of the faulty ASS considering its parameter uncertainties is described as

$$\begin{cases} \dot{\boldsymbol{x}}_f(t) = \sum_{i=1}^{8} h_i(\xi(t)) \begin{pmatrix} \boldsymbol{A}_i\boldsymbol{x}_f(t) + \boldsymbol{B}_i(\boldsymbol{u}_f(t) \\ +f(t)) + \boldsymbol{B}_{1i}\boldsymbol{w}(t) \end{pmatrix} \\ \boldsymbol{y}_f(t) = \sum_{i=1}^{8} h_i(\xi(t)) \begin{pmatrix} \boldsymbol{C}_i\boldsymbol{x}_f(t) + \boldsymbol{D}_i(\boldsymbol{u}_f(t) \\ +f(t) \end{pmatrix} \\ \boldsymbol{z}_f(t) = \sum_{i=1}^{8} h_i(\xi(t)) \begin{pmatrix} \boldsymbol{C}_{1i}\boldsymbol{x}_f(t) + \boldsymbol{D}_{1i}(\boldsymbol{u}_f(t) \\ +f(t) + \boldsymbol{E}_{1i}\boldsymbol{w}(t) \end{pmatrix} \end{cases} \tag{9}$$

where $\boldsymbol{f}(t)$ is the deviation quantity between the desirable control force and the real output force generated by the actuator, and it is commonly expressed as an intermittent or continuous signal. Besides, $\boldsymbol{x}_f(t)$, $\boldsymbol{y}_f(t)$, and $\boldsymbol{z}_f(t)$ denote the corresponding the system state vector, the sytem output vector and the control output vector of the control plant. Here, two types of fault signals are considered in the simulation investigations and discussions at Section 4, the former one is an abrupt fault, and the latter one is named as a time-varying fault.

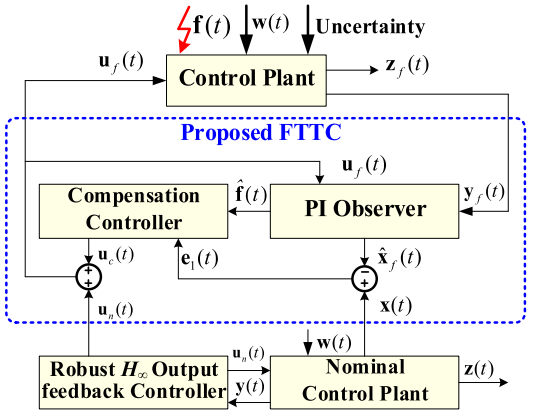

FIGURE 4. Fault tolerant tracking controller scheme.

Remark 2: It is a fact that the actuator faults is a critical and fairly common fault scenario in ASS. and compared with the other parts in vehicle chassis system, the occurrence probability of the actuator faults is higher and more serious. Moreover, it should be noticed that componment catastrophic failures, unknown external disturbances, system parameter variations, degradations and partial blockages are usually believed to cause the actuator deviation fault [30], which means the actuator will generate insufficient or excessive control force.

Herein, to reveal the approximation effect of T-S fuzzy model applied to this half-vehicle ASS, the state error curve of T-S fuzzy system approximating the ASS is shown in Fig. 3, wherein $\boldsymbol{x_j}$ (j= 1, . . . , 8) represents $z_c\,(t)$, $\dot{z}_c\,(t)$, $\phi\,(t)$, $\dot{\phi}\,(t)$, $z_{uf}\,(t)$, $z_{ur}\,(t)$, $\dot{z}_{uf\,(t)}$, and $\dot{z}_{ur}\,(t)$, respectively.

It is obvious from Fig. 3 that, T-S fuzzy model of the ASS can closely approximate the real model of the ASS, and the approximation errors of each state of the ASS are controlled below ± 0.005, meeting the error accuracy requirements.

C. CONTROL PROBLEM STATEMENT

The main control objectives in this work are generalized as follows:

(1) The proposed FTTC can guarantee the minimization of $|\ddot{z}_c\,(t)|$ and $\ddot{\phi}\,(t)$ for the uncertain ASS in case of the actuator faults and unknown road disturbances.

(2) The following hard constraints are expected to be satisfied as follows:

- The ratio of tire dynamical loads versus their static loads at the front and rear wheel (denoted by F^f_{ratio} and F^r_{ratio}, respectively) should be less than one, which is given by

$$\begin{cases} F^f_{\text{ratio}} = \dfrac{|k_{tf}\,(z_{uf} - z_{rf})|}{F_{ff}} < 1 \\ F^r_{\text{ratio}} = \dfrac{|k_{tr}\,(z_{ur} - z_{rr})|}{F_{fr}} < 1 \end{cases} \tag{10}$$

where F_{ff} and F_{fr} are calculated by

$$\begin{cases} F_{ff} + F_{fr} = (m_s + m_{uf} + m_{ur})g \\ F_{ff}(a+b) = m_s g b + m_{uf} g(a+b) \end{cases} \tag{11}$$

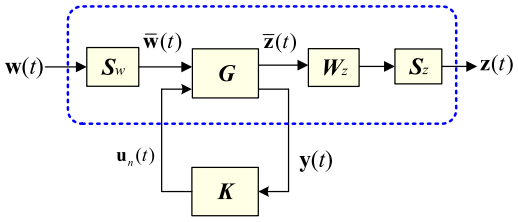

FIGURE 5. The ROFC diagram under the fault-free condition.

Note that $g = 9.8\text{N}/m^2$, and it is easily calculated by (11) that $F_{ff} = 7224.1\text{N}$, $F_{fr} = 5859.3\text{N}$.

- The desirable control forces of the FR wheel's actuators should be less than their corresponding limits as $u\,(t)_{Ff\_max}$ and $u\,(t)_{Fr\_max}$, which are given by

$$\begin{cases} |u_{Ff}\,(t)| \le u_{Ff\_max} \\ |u_{Fr}\,(t)| \le u_{Fr\_max} \end{cases} \tag{12}$$

(3) When facing the actuator fault, it is expected that the ride quality and handling stability of ASS with the actuator are almost the same as those of ASS without the actuator failures.

To facilitate the subsequent controller design, it is necessary to present the following three assumptions and lemmas [31], [32].

Assumption 1: The external unknown disturbance $w(t)$ should satisfy $\|w(t)\| \le \bar{d}$, where $\bar{d} > 0$ is an unknown constant.

Assumption 2: There exists one positive constant $u_{f\_\max} = 1500\text{N}$ [33] such that for the control force $\boldsymbol{u}_f(t)$, $\|\boldsymbol{u}_f(t)\| \le u_{f\_\max}$ is satisfied.

Assumption 3: Without losing universality, $\boldsymbol{f}(t)$ is considered to be satisfied with $\|\boldsymbol{f}(t)\| \le f_\lambda$, where f_λ is an unknown positive constant.

Based on Assumption 1 to Assumption 3, we can logically get Remark 3 as follows:

Remark 3: In terms of Assumption 1 and Assumption 2, it is easily observed that the real control forces and external disturbance are all bounded. When the ASS works without actuator faults, it is a reasonable assumption to make in most actual systems. Additionally, Assumption 3 indicates that the actuator fault is restrained within a certain range. This assumption is effective except for the breakpoint of sudden failure that are not considered in this work, and the same assumption can be found in [24] and [34].

Lemma 1: Consider the following common linear time-invariant system:

$$\begin{cases} \dot{\boldsymbol{x}}(t) = \boldsymbol{A}\boldsymbol{x}(t) + \boldsymbol{B}\boldsymbol{w}(t) \\ \boldsymbol{z}(t) = \boldsymbol{C}\boldsymbol{x}(t) + \boldsymbol{D}\boldsymbol{w}(t) \end{cases} \tag{13}$$

Given a positive constant β, if there exists a positive definite matrix $\boldsymbol{Q} > 0$ satisfying

$$\begin{bmatrix} \boldsymbol{A}^T\boldsymbol{Q} + \boldsymbol{Q}\boldsymbol{A} & \boldsymbol{Q}\boldsymbol{B} & \boldsymbol{C}^T \\ * & -\beta\boldsymbol{I} & \boldsymbol{D}^T \\ * & * & -\beta\boldsymbol{I} \end{bmatrix} \tag{14}$$

Then, the closed-loop system (13) will approach an asymptotical steady state, and $\|z(t)\|_2 \leq \beta \|w(t)\|_2$ holds under the zero initial condition.

III. FAULT-TOLERANT TRACKING CONTROLLER SYNTHESIS

In this section, Fig. 4 is used to describe the control idea and framework of the proposed PIO-based FTTC controller for the faulty uncertain ASS.

In this paper, considering normal suspension system and fault suspension system, our goal is to design a compound fault-tolerant tracking controller based on PI observer (PIO-FTTC), which meets the following requirements:

(1) First, we design a robust output feedback control (ROFC) for the normal suspension system to ensure the control performance of the active suspension system during normal operation. The normal operation control force of ROFC is expressed as $\boldsymbol{u}_n(t)$, and the output performance index controlled by the normal suspension system is used as an ideal reference trajectory. (2) Meanwhile, when the suspension system fails, a PI observer is designed to estimate the state $\boldsymbol{x}_f(t)$ of the fault suspension system and the fault signal $\boldsymbol{f}(t)$, and the amplitude of the fault signal is calculated according to $\boldsymbol{y}_f(t)$. The fault estimation signal is feed back to the fault tolerant controller (FTC) designed by us, and the compensation control force $\boldsymbol{u}_c(t)$ is output. The superimposed fault suspension control force $\boldsymbol{u}_f(t)$ is input to the fault suspension system, so as to achieve the fault compensation control and stabilize the performance of the fault suspension system.

A. ROBUST H_∞ OUTPUT FEEDBACK CONTROLLER

As for the control system with model uncertainties and without actuator faults, the ROFC is an effective control strategy to maintain good performances for this ASS, in which the $\boldsymbol{H}_\infty$ norm between the interference input and the control output vector is regarded as the optimization goal to satisfy the hard constraints. In general, the diagram of the nominal ROFC is presented in Fig. 5.

In Fig. 5, $\boldsymbol{S}_w$ is the weighted coefficient matrix of $\boldsymbol{w}(t)$, $\boldsymbol{G}$ is the transfer function of system (8), $\boldsymbol{K}$ is the determined gain matrix of the ROFC, $\boldsymbol{W}_z$ and $\boldsymbol{S}_z$ are the coefficient matrixes of the road disturbance input and the control output $\boldsymbol{z}(t)$, respectively. $\bar{\boldsymbol{w}}(t)$ and $\bar{\boldsymbol{z}}(t)$ represent the weighted signals of $\boldsymbol{w}(t)$ and $\boldsymbol{z}(t)$, respectively. Additionally, $\boldsymbol{u_n}(t)$ is the control law of the ROFC, and the $\boldsymbol{H}_\infty$ norm $\|T_{zw}(t)\|_\infty$ of $\boldsymbol{w}(t)$ versus $\boldsymbol{z}(t)$ is bounded by β, i.e., $\|T_{zw}(t)\|_\infty = \sup_{w\in L_2} \frac{\|z(t)\|_2}{\|w(t)\|_2} < \beta$, where β is a positive constant.

By further derivations, one can get a state space equation as follows:

$$\begin{cases} \dot{\boldsymbol{x}}_c(t) = \boldsymbol{A}_c \boldsymbol{x}_c(t) + \boldsymbol{B}_c \boldsymbol{y}(t) \\ \boldsymbol{u}_n(t) = \boldsymbol{C}_c \boldsymbol{x}_c(t) + \boldsymbol{D}_c \boldsymbol{y}(t) \end{cases} \tag{15}$$

where $\boldsymbol{x}_c(t)$ is the state vector of the nominal control plant, and $\boldsymbol{A}_c, \boldsymbol{B}_c, \boldsymbol{C}_c$ and $\boldsymbol{D}_c$ represent the parameter matrices of the ROFC, respectively.

Synthesizing Eq. (8) and Eq. (15) generates

$$\begin{cases} \dot{\boldsymbol{x}}_{cl}(t) = \sum_{i=1}^{8} h_i \left(\boldsymbol{A}_{ci} \boldsymbol{x}_{cl}(t) + \boldsymbol{B}_{ci} \boldsymbol{w}(t) \right) \\ \boldsymbol{z}(t) = \sum_{i=1}^{8} h_i \left(\boldsymbol{C}_{ci} \boldsymbol{x}_{cl}(t) + \boldsymbol{D}_{ci} \boldsymbol{w}(t) \right) \end{cases} \tag{16}$$

where $\boldsymbol{x}_{cl}(t) = [\boldsymbol{x}(t), \boldsymbol{x}_c(t)]^T$ is the state vector, and the corresponding coefficient matrices are derived as:

$$\boldsymbol{A}_{ci} = \begin{bmatrix} \boldsymbol{A}_i + \boldsymbol{B}_i \boldsymbol{D}_c \boldsymbol{C}_i & \boldsymbol{B}_i \boldsymbol{C}_c \\ \boldsymbol{B}_c \boldsymbol{C}_i & \boldsymbol{A}_c \end{bmatrix}, \quad \boldsymbol{B}_{ci} = \begin{bmatrix} \boldsymbol{B}_{1i} \\ 0 \end{bmatrix},$$
$$\boldsymbol{C}_{ci} = \begin{bmatrix} \boldsymbol{C}_{1i} + \boldsymbol{D}_{1i} \boldsymbol{D}_c \boldsymbol{C}_i & \boldsymbol{D}_{1i} \boldsymbol{C}_c \end{bmatrix}, \quad \boldsymbol{D}_{ci} = [\boldsymbol{E}_{1i}].$$

Thus far, the control goal is to find out the appropriate coefficient matrices $\boldsymbol{A}_{ci}, \boldsymbol{B}_{ci}, \boldsymbol{C}_{ci}$ and $\boldsymbol{D}_{ci}$ and thus the desired controller can be obtained and the asymptotic stability of system (16) can aslo be ensured. Based on **Lemma 1**, the necessary and sufficient condition of this designed ROFC is that there exists a symmetric positive definite matrix $\mathbf{Q}$ such that

$$\begin{bmatrix} \boldsymbol{A}_{ci}^T \boldsymbol{Q} + \boldsymbol{Q} \boldsymbol{A}_{ci}^T & \boldsymbol{Q} \boldsymbol{B}_{ci} & \boldsymbol{C}_{ci}^T \\ * & -\beta \boldsymbol{I} & \boldsymbol{D}_{ci} \\ * & * & -\beta \boldsymbol{I} \end{bmatrix} \tag{17}$$

In terms of $\boldsymbol{S}_w, \boldsymbol{W}_z, \boldsymbol{S}_z$, we can calculate $\boldsymbol{A}_c, \boldsymbol{B}_c, \boldsymbol{C}_c$ and $\boldsymbol{D}_c$ by using MATLAB internal function 'hinflmi', and further obtain $\boldsymbol{u}_n(t)$ through (15). Afterwards, substituting $\boldsymbol{A}_c, \boldsymbol{B}_c, \boldsymbol{C}_c$ and $\boldsymbol{D}_c$ into $\boldsymbol{A}_{ci}, \boldsymbol{B}_{ci}, \boldsymbol{C}_{ci}$ and $\boldsymbol{D}_{ci}$ yields (16).

B. PIO-BASED FAULT-TOLERANT TRACKING CONTROLLER SYNTHESIS

Based on the above discussions, this section introduces the design of a PIO-based FTTC such that the output performances of the faulty ASS can converge to a specified trajectory within a finite time. So, the following fault-tolerant control law $\boldsymbol{u}_f(t)$ is considered as

$$\boldsymbol{u}_f(t) = \boldsymbol{u}_n(t) + \boldsymbol{u}_c(t) \tag{18}$$

where $\boldsymbol{u}_c(t) = -\hat{\boldsymbol{f}}(t) + \boldsymbol{K}_{1i} \boldsymbol{e}_1(t)$ denotes the compensation control force, $\boldsymbol{e}_1(t) = \boldsymbol{x}(t) - \hat{\boldsymbol{x}}_f(t)$ and $\boldsymbol{K}_{1i}$ stand for the undetermined state feedback gain matrix, $\hat{\boldsymbol{f}}(t)$ and $\hat{\boldsymbol{x}}_f(t)$ are the estimation of the fault signal and state variables via PIO, respectively.

To derive the desirable FTC law, the general form of PIO is designed as

$$\begin{cases} \dot{\hat{\boldsymbol{x}}}_f(t) = \sum_{i=1}^{8} h_i \begin{pmatrix} \boldsymbol{A}_i \hat{\boldsymbol{x}}_f(t) + \boldsymbol{B}_i \left(\boldsymbol{u}_f(t) + \hat{\boldsymbol{f}}(t) \right) \\ + \boldsymbol{H}_{1i} \left(\boldsymbol{y}_f(t) - \hat{\boldsymbol{y}}_f(t) \right) \end{pmatrix} \\ \hat{\boldsymbol{y}}_f(t) = \sum_{i=1}^{8} h_i \left(\boldsymbol{C}_i \hat{\boldsymbol{x}}_f(t) + \boldsymbol{D}_i \left(\boldsymbol{u}_f(t) + \hat{\boldsymbol{f}}(t) \right) \right) \\ \dot{\hat{\boldsymbol{f}}}(t) = \sum_{i=1}^{8} h_i \left(\boldsymbol{H}_{2i} \left(\boldsymbol{y}_f(t) - \hat{\boldsymbol{y}}_f(t) \right) \right) \end{cases} \tag{19}$$

where $\boldsymbol{H}_{1i}$ and $\boldsymbol{H}_{2i}$ are the determined gain matrices of the PIO used for estimating $\boldsymbol{f}(t)$ and $\boldsymbol{x_f}(t)$, respectively. By using

this proposed FTTC strategy, it can be pointed out that the fault detection and isolation are based on accurate estimation of PIO for the actuator fault in (19). Moreover, the designed PIO can estimate $\ddot{z}_c\ddot{\phi}(t)$, Δy_f, Δy_r, F_{ff}, F_{fr}, u_{Ff} and u_{Fr}, respectively. It is noted that the inputs of this PIO are $\boldsymbol{u}_f(t)$ and $\boldsymbol{y}_f(t)$, and the outputs of this PIO are $\hat{\boldsymbol{x}}_f(t)$ and $\hat{\boldsymbol{f}}(t)$.

1) FTTC DESIGN FOR THE ABRUPT FAULT

Firstly, we think that the actuator failure affecting the vehicle suspension system is based on the abrupt fault with $\boldsymbol{f}(t) = c$ [35], where $c \in R$, then the output error between (9) and (19) is written by.

$$\boldsymbol{y}_f(t) - \hat{\boldsymbol{y}}_f(t) = \sum_{i=1}^{8} h_i\left(\tilde{\boldsymbol{C}}_i \boldsymbol{e}_a(t)\right) \tag{20}$$

where $\boldsymbol{y}_f(t)$ and $\hat{\boldsymbol{y}}_f(t)$are defined in (9) and (19), respectolively, $\tilde{\boldsymbol{C}}_i = \begin{bmatrix}\boldsymbol{C}_i & \boldsymbol{D}_i\end{bmatrix}$, $\boldsymbol{e}_a(t) = \boldsymbol{x}_a(t) - \hat{\boldsymbol{x}}_a(t) = \begin{bmatrix}\boldsymbol{x}_f(t) - \hat{\boldsymbol{x}}_f(t) \\ \boldsymbol{f}(t) - \hat{\boldsymbol{f}}(t)\end{bmatrix}$, and $\boldsymbol{x}_a(t) = \begin{bmatrix}\boldsymbol{x}_f(t) \\ \boldsymbol{f}(t)\end{bmatrix}$, $\hat{\boldsymbol{x}}_a(t) = \begin{bmatrix}\hat{\boldsymbol{x}}_f(t) \\ \hat{\boldsymbol{f}}(t)\end{bmatrix}$.

Define $\tilde{\boldsymbol{L}} = \begin{bmatrix}\boldsymbol{B}_i\boldsymbol{K}_{1i} & \boldsymbol{B}_i\end{bmatrix}$, the dynamic tracking error $\boldsymbol{e}_2(t) = \boldsymbol{x}(t) - \boldsymbol{x}_f(t)$ is then given by

$$\begin{aligned}
&\dot{\boldsymbol{e}}_2(t) \\
&= \sum_{i=1}^{8} h_i \begin{pmatrix} \boldsymbol{A}_i\boldsymbol{x}(t) + \boldsymbol{B}_i\boldsymbol{u}_n(t) + \boldsymbol{B}_{1i}\boldsymbol{w}(t) \\ -\left(\boldsymbol{A}_i\boldsymbol{x}_f(t) + \boldsymbol{B}_i\left(\boldsymbol{u}_f(t) + \boldsymbol{f}(t)\right) + \boldsymbol{B}_{1i}\boldsymbol{w}(t)\right) \end{pmatrix} \\
&= \sum_{i=1}^{8} h_i \begin{pmatrix} \boldsymbol{A}_i\boldsymbol{e}_2(t) + \boldsymbol{B}_i\left(\boldsymbol{u}_f(t) + \hat{\boldsymbol{f}}(t)\right) \\ -\boldsymbol{B}_i\boldsymbol{K}_{1i}\left(\boldsymbol{x}(t) - \hat{\boldsymbol{x}}_f(t)\right) - \boldsymbol{B}_i\boldsymbol{u}_f(t) - \boldsymbol{B}_i\boldsymbol{f}(t) \end{pmatrix} \\
&= \sum_{i=1}^{8} h_i \begin{pmatrix} \boldsymbol{A}_i\boldsymbol{e}_2(t) - \boldsymbol{B}_i\left(\boldsymbol{f}(t) - \hat{\boldsymbol{f}}(t)\right) \\ -\boldsymbol{B}_i\boldsymbol{K}_{1i}\left(\boldsymbol{x}_f(t) - \hat{\boldsymbol{x}}_f(t)\right) \end{pmatrix} \\
&= \sum_{i=1}^{8} h_i\left(\boldsymbol{A}_i\boldsymbol{e}_2(t) - \tilde{\boldsymbol{L}}\boldsymbol{e}_a(t)\right)
\end{aligned} \tag{21}$$

The derivative of the state errors $\dot{\boldsymbol{e}}_a(t)$ is written as

$$\dot{\boldsymbol{e}}_a(t) = \sum_{i=1}^{8} h_i\left(\left(\bar{\boldsymbol{A}}_i - \bar{\boldsymbol{H}}_i\tilde{\boldsymbol{C}}_i\right)\boldsymbol{e}_a(t) + \bar{\boldsymbol{B}}_{1i}\boldsymbol{w}(t)\right) \tag{22}$$

where

$$\bar{\boldsymbol{A}}_i = \begin{bmatrix}\boldsymbol{A}_i & \boldsymbol{B}_i \\ 0 & 0\end{bmatrix}, \quad \bar{\boldsymbol{H}}_i = \begin{bmatrix}\boldsymbol{H}_{1i} \\ \boldsymbol{H}_{2i}\end{bmatrix},$$
$$\tilde{\boldsymbol{C}}_i = \begin{bmatrix}\boldsymbol{C}_i & \boldsymbol{D}_i\end{bmatrix}, \quad \bar{\boldsymbol{B}}_{1i} = \begin{bmatrix}\boldsymbol{B}_{1i} \\ 0\end{bmatrix}.$$

Synthesizing (21) and (22) generates the augmentation system of dynamic tracking errors system as

$$\dot{\tilde{\boldsymbol{e}}}(t) = \sum_{i=1}^{8} h_i\left(\tilde{\boldsymbol{A}}_i\tilde{\boldsymbol{e}}(t) + \tilde{\boldsymbol{B}}_{1i}\boldsymbol{w}(t)\right) \tag{23}$$

where

$$\tilde{\boldsymbol{e}}(t) = \begin{bmatrix}\boldsymbol{e}_2(t) \\ \boldsymbol{x}_f(t) - \hat{\boldsymbol{x}}_f(t) \\ \boldsymbol{f}(t) - \hat{\boldsymbol{f}}(t)\end{bmatrix},$$

$$\tilde{\boldsymbol{A}}_i = \begin{bmatrix}\boldsymbol{A}_i & -\boldsymbol{B}_i\boldsymbol{K}_{1i} & -\boldsymbol{B}_i \\ 0 & \boldsymbol{A}_i - \boldsymbol{H}_{1i}\boldsymbol{C}_i & \boldsymbol{B}_i - \boldsymbol{H}_{1i}\boldsymbol{D}_i \\ 0 & -\boldsymbol{H}_{2i}\boldsymbol{C}_i & -\boldsymbol{H}_{2i}\boldsymbol{D}_i\end{bmatrix}, \quad \tilde{\boldsymbol{B}}_{1i} = \begin{bmatrix}0 \\ \boldsymbol{B}_{1i} \\ 0\end{bmatrix}$$

Based on (23), the design of FTTC can be converted into solving the gain matrices $\boldsymbol{H}_{1i}$, $\boldsymbol{H}_{2i}$ of PIO and the state feedback gain matrices $\boldsymbol{K}_{1i}$ of the FTTC, which meet the following performance requirements:

(1) The system (24) is asymptotically stable;

(2) Under zero initial conditions, $\forall \boldsymbol{w}(t) \in L_2[0, +\infty)$, supposed that the transfer function from $\boldsymbol{w}(t)$ to $\tilde{\boldsymbol{e}}(t)$ is $T_{\tilde{\boldsymbol{e}}\boldsymbol{w}}(t)$, solving $\boldsymbol{H}_{1i}, \boldsymbol{H}_{2i}$ and $\boldsymbol{K}_{1i}$ can make the system (23) satisfying $\boldsymbol{H}_\infty$ performance index $\|T_{\tilde{\boldsymbol{e}}\boldsymbol{w}}(t)\|_\infty < \gamma$, i.e.

$$\|T_{\tilde{\boldsymbol{e}}\boldsymbol{w}}(t)\|_\infty = \sup_{w \in L2} \frac{\|\tilde{\boldsymbol{e}}(t)\|_2}{\|\boldsymbol{w}(t)\|_2} < \gamma \tag{24}$$

Based on the aforementioned derivations, the proposed FTTC design can be generalized as Theorem 1.

Theorem 1. The system (23) is asymptotically stable, and the $\boldsymbol{H}_\infty$ performance index $\|T_{\tilde{\boldsymbol{e}}\boldsymbol{w}}(t)\|_\infty < \gamma$ defined in (25) can be guaranteed under zero initial condition, if there exist symmetrical matrices $\boldsymbol{H}_{1i}, \boldsymbol{H}_{2i}, \boldsymbol{K}_{1i}, \boldsymbol{P}_1, \gamma > 0$, and the positive symmetrical matrices $\boldsymbol{X}_1 > 0$, $\boldsymbol{P}_2 > 0$, along with $\boldsymbol{P}_3 = \boldsymbol{I}$.Therefore, the following convex optimization problem hold:

$$\min_{\boldsymbol{X}_1, \boldsymbol{P}_2, \boldsymbol{K}_{1i}, \boldsymbol{H}_{1i}, \boldsymbol{H}_{2i}} \gamma$$
$$\text{s.t.} \quad \begin{bmatrix} \boldsymbol{\xi}_i & \boldsymbol{P}\tilde{\boldsymbol{B}}_{1i} & \boldsymbol{\Gamma} & -\boldsymbol{Q}_i & -\boldsymbol{W} \\ * & -\gamma\boldsymbol{I} & 0 & 0 & 0 \\ * & * & -\gamma\boldsymbol{I} & 0 & 0 \\ * & * & * & -\boldsymbol{I} & 0 \\ * & * & * & * & -\boldsymbol{I} \end{bmatrix} < 0 \tag{25}$$

where $\boldsymbol{\xi}_i = \tilde{\boldsymbol{A}}_i^T\boldsymbol{P} + \boldsymbol{P}\tilde{\boldsymbol{A}}_i - \boldsymbol{Q}_i\boldsymbol{W}^T - \boldsymbol{W}\boldsymbol{Q}_i^T$, $\boldsymbol{Q}_i = \begin{bmatrix}\boldsymbol{B}_i\boldsymbol{K}_{1i} & 0 & 0\end{bmatrix}^T$, $\boldsymbol{W} = \begin{bmatrix}\boldsymbol{X}_1 & 0 & 0\end{bmatrix}^T$, $\boldsymbol{\Gamma} = \begin{bmatrix}\boldsymbol{X}_1 & \boldsymbol{I} & \boldsymbol{I}\end{bmatrix}^T$, $\boldsymbol{P} = \text{diag}\left\{\boldsymbol{P}_1, \boldsymbol{P}_2, \boldsymbol{P}_3\right\}$, $\boldsymbol{P} = \boldsymbol{P}^T > 0$.

Proof: Define the Lyapunov function as

$$\boldsymbol{V}(t) = \tilde{\boldsymbol{e}}^T(t)\boldsymbol{P}\tilde{\boldsymbol{e}}(t) \tag{26}$$

Taking the derivation of $\boldsymbol{V}(t)$ along t and incorporating (23) give

$$\begin{aligned}
\dot{\boldsymbol{V}}(t) = \sum_{i=1}^{8} h_i(\tilde{\boldsymbol{e}}^T(t)\left(\tilde{\boldsymbol{A}}_i^T\boldsymbol{P} + \boldsymbol{P}\tilde{\boldsymbol{A}}_i\right)\tilde{\boldsymbol{e}}(t) \\
+ \boldsymbol{w}^T(t)\tilde{\boldsymbol{B}}_{1i}^T\boldsymbol{P}\tilde{\boldsymbol{e}}(t) + \tilde{\boldsymbol{e}}^T(t)\boldsymbol{P}\tilde{\boldsymbol{B}}_{1i}\boldsymbol{w}(t)
\end{aligned} \tag{27}$$

Considering $\boldsymbol{w}(t)$ as the disturbance input, and according to [13], the $\boldsymbol{H}_\infty$ performance index of this control plant, $T_{\tilde{\boldsymbol{e}}\boldsymbol{w}}(t)$ is defined as

$$\|T_{\tilde{\boldsymbol{e}}\boldsymbol{w}}(t)\|_\infty = \sup_{w \in L_2} \frac{\|\tilde{\boldsymbol{e}}(t)\|_2}{\|\boldsymbol{w}(t)\|_2} < \gamma \tag{28}$$

Note that (28) can be equivalently transformed into

$$\int_0^t \left(\frac{1}{\gamma}\tilde{\boldsymbol{e}}^T(t)\tilde{\boldsymbol{e}}(t) - \gamma\boldsymbol{w}(t)^T\boldsymbol{w}(t)\right)dt < 0 \tag{29}$$

To guarantee that system (23) is asymptotically stable, i.e., $\dot{V}(t) < 0$, synthesizing (27) and (29) yields

$$\int_0^t \left(\begin{bmatrix} \tilde{\boldsymbol{e}}(t) \\ \boldsymbol{w}(t) \end{bmatrix}^T \times \begin{bmatrix} \tilde{\boldsymbol{A}}_i^T \boldsymbol{P} + \boldsymbol{P}\tilde{\boldsymbol{A}}_i + \frac{1}{\gamma}\boldsymbol{I} & \boldsymbol{P}\tilde{\boldsymbol{B}}_{1i} \\ * & -\gamma \boldsymbol{I} \end{bmatrix} \times \begin{bmatrix} \tilde{\boldsymbol{e}}(t) \\ \boldsymbol{w}(t) \end{bmatrix} \right) dt < 0 \tag{30}$$

If

$$\begin{bmatrix} \tilde{\boldsymbol{A}}_i^T \boldsymbol{P} + \boldsymbol{P}\tilde{\boldsymbol{A}}_i + \frac{1}{\gamma}\boldsymbol{I} & \boldsymbol{P}\tilde{\boldsymbol{B}}_{1i} \\ * & -\gamma \boldsymbol{I} \end{bmatrix} < 0 \tag{31}$$

Then, system (23) is asymptotically stable satisfying $\|T_{\tilde{e}\boldsymbol{w}}(t)\|_\infty =< \gamma$.

Applying Schur complement lemma to (31), we have

$$\begin{bmatrix} \tilde{\boldsymbol{A}}_i^T \boldsymbol{P} + \boldsymbol{P}\tilde{\boldsymbol{A}}_i & \boldsymbol{P}\tilde{\boldsymbol{B}}_{1i} & \boldsymbol{I} \\ * & -\gamma \boldsymbol{I} & 0 \\ * & * & -\gamma \boldsymbol{I} \end{bmatrix} \tag{32}$$

By expanding the corresponding coefficient matrices of (32), we get

$$\begin{bmatrix} \boldsymbol{J}_i & -\boldsymbol{P}_1\boldsymbol{B}_i\boldsymbol{K}_{1i} & -\boldsymbol{P}_1\boldsymbol{B}_i & 0 & \boldsymbol{I} & 0 & 0 \\ * & \boldsymbol{\Omega}_i & \boldsymbol{\Delta}_i & \boldsymbol{P}_2\boldsymbol{B}_{1i} & 0 & \boldsymbol{I} & 0 \\ * & * & \boldsymbol{\chi}_i & 0 & 0 & 0 & \boldsymbol{I} \\ * & * & * & -\gamma \boldsymbol{I} & 0 & 0 & 0 \\ * & * & * & * & -\gamma \boldsymbol{I} & 0 & 0 \\ * & * & * & * & * & -\gamma \boldsymbol{I} & 0 \\ * & * & * & * & * & * & -\gamma \boldsymbol{I} \end{bmatrix} \tag{33}$$

where

$$\begin{aligned} \boldsymbol{J}_i &= \boldsymbol{P}_1\boldsymbol{A}_i + \boldsymbol{A}_i^T\boldsymbol{P}_1 - \boldsymbol{P}_1\boldsymbol{B}_i\boldsymbol{K}_{1i} - \boldsymbol{K}_{1i}^T\boldsymbol{B}_i^T\boldsymbol{P}_1, \\ \boldsymbol{\Omega}_i &= \boldsymbol{P}_2\boldsymbol{A}_i + \boldsymbol{A}_i^T\boldsymbol{P}_2 - \bar{\boldsymbol{H}}_{1i}\boldsymbol{C}_i - \boldsymbol{C}_i^T\bar{\boldsymbol{H}}_{1i}^T, \\ \boldsymbol{\Delta}_i &= \boldsymbol{P}_2\boldsymbol{B}_i - \bar{\boldsymbol{H}}_{1i}\boldsymbol{R}_i - \boldsymbol{C}_i^T\boldsymbol{H}_{2i}^T, \\ \boldsymbol{\chi}_i &= -\bar{\boldsymbol{H}}_{2i}\boldsymbol{R}_i - \boldsymbol{R}_i^T\bar{\boldsymbol{H}}_{2i}^T, \\ \bar{\boldsymbol{H}}_{1i} &= \boldsymbol{P}_2\boldsymbol{H}_{1i} \quad \text{and} \quad \bar{\boldsymbol{H}}_{2i} = \boldsymbol{P}_3\boldsymbol{H}_{2i}. \end{aligned}$$

Pre- and post- multiplying (33) by *diag* $\{\boldsymbol{P}_1^{-1}, \mathbf{I}, \mathbf{I}, \mathbf{I}, \mathbf{I}, \mathbf{I}, \mathbf{I}\}$ and *diag* $\{\boldsymbol{P}_1^{-1}, \mathbf{I}, \mathbf{I}, \mathbf{I}, \mathbf{I}, \mathbf{I}, \mathbf{I}\}$, then (33) is transformed into

$$\begin{bmatrix} \boldsymbol{\varphi}_i & -\boldsymbol{B}_i\boldsymbol{K}_{1i} & -\boldsymbol{B}_i & 0 & \boldsymbol{X}_1 & 0 & 0 \\ * & \boldsymbol{\Omega}_i & \boldsymbol{\Delta}_i & \boldsymbol{P}_2\boldsymbol{B}_{1i} & 0 & \boldsymbol{I} & 0 \\ * & * & \boldsymbol{\chi}_i & 0 & 0 & 0 & \boldsymbol{I} \\ * & * & * & -\gamma \boldsymbol{I} & 0 & 0 & 0 \\ * & * & * & * & -\gamma \boldsymbol{I} & 0 & 0 \\ * & * & * & * & * & -\gamma \boldsymbol{I} & 0 \\ * & * & * & * & * & * & -\gamma \boldsymbol{I} \end{bmatrix} < 0 \tag{34}$$

Substitute $\boldsymbol{\varphi}_{ij} = \boldsymbol{A}_i\boldsymbol{X}_1 + \boldsymbol{X}_1\boldsymbol{A}_i^T - \boldsymbol{B}_i\boldsymbol{K}_{1i}\boldsymbol{X}_1 - \boldsymbol{X}_1\boldsymbol{K}_{1i}^T\boldsymbol{B}_i^T$ and $\boldsymbol{X}_1 = \boldsymbol{P}_1^{-1}$ into (34), we obtain (35), as shown at the bottom of the next page. After further transformation, we have (36), as shown at the bottom of the next page.

TABLE 1. The parameters of half ASS model.

parameter	value
I_y	1713 kg·m^2
k_f	22741 N·m^{-1}
k_r	22741 N·m^{-1}
k_{tf}	492982 N·m^{-1}
k_{tr}	302342 N·m^{-1}
c_f	1221 N·s·m^{-1}
c_r	1228 N·s·m^{-1}
a	1.2 m
b	1.5 m

By defining $\boldsymbol{\eta}_i = \begin{bmatrix} \boldsymbol{A}_i\boldsymbol{X}_1 + \boldsymbol{X}_1\boldsymbol{A}_i^T & -\boldsymbol{B}_i\boldsymbol{K}_{1i} & -\boldsymbol{B}_i \\ * & \boldsymbol{\Omega}_i & \boldsymbol{\Delta}_i \\ * & * & \boldsymbol{\chi}_i \end{bmatrix}$, $\tilde{\boldsymbol{B}}_{1i} = \begin{bmatrix} 0 \\ \boldsymbol{B}_{1i} \\ 0 \end{bmatrix}$ and $\boldsymbol{\sigma} = \begin{bmatrix} \boldsymbol{X}_1 & 0 & 0 \\ 0 & \boldsymbol{I} & 0 \\ 0 & 0 & \boldsymbol{I} \end{bmatrix}$, the above (36) can be transformed as

$$\begin{bmatrix} \boldsymbol{\eta}_i & \boldsymbol{P}\tilde{\boldsymbol{B}}_{1i} & \boldsymbol{\sigma} \\ * & -\gamma \boldsymbol{I} & 0 \\ * & * & -\gamma \boldsymbol{I} \end{bmatrix} - \begin{bmatrix} \boldsymbol{B}_i\boldsymbol{K}_{1i}\boldsymbol{X}_1 + \boldsymbol{X}_1\boldsymbol{K}_{1i}^T\boldsymbol{B}_i^T & 0 & 0 & 0 & 0 & 0 & 0 \\ 0 & 0 & 0 & 0 & 0 & 0 & 0 \\ 0 & 0 & 0 & 0 & 0 & 0 & 0 \\ 0 & 0 & 0 & 0 & 0 & 0 & 0 \\ 0 & 0 & 0 & 0 & 0 & 0 & 0 \\ 0 & 0 & 0 & 0 & 0 & 0 & 0 \\ 0 & 0 & 0 & 0 & 0 & 0 & 0 \end{bmatrix} < 0 \tag{37}$$

Note that (37) can be further rewritten as

$$\begin{bmatrix} \boldsymbol{\eta}_i & \boldsymbol{P}\tilde{\boldsymbol{B}}_{1i} & \boldsymbol{\sigma} \\ * & -\gamma \boldsymbol{I} & 0 \\ * & * & -\gamma \boldsymbol{I} \end{bmatrix} - \left(\begin{bmatrix} \boldsymbol{Q}_i \\ 0 \\ 0 \end{bmatrix} \begin{bmatrix} \boldsymbol{W} \\ 0 \\ 0 \end{bmatrix}^T + \begin{bmatrix} \boldsymbol{W} \\ 0 \\ 0 \end{bmatrix} \begin{bmatrix} \boldsymbol{Q}_i \\ 0 \\ 0 \end{bmatrix}^T \right) < 0 \tag{38}$$

Using Schur complement lemma again, (38) is then transformed into (25), thus Theorem 1 is proved.

2) FTTC DESIGN FOR THE TIME-VARYING FAULT

For the time-varying fault, it is assumed that $\boldsymbol{f}(t) = d + he^{kt}$ on basis of Assumption 3 and [36], wherein $d, h, k \in R$, then it is easy to obtain $\tilde{\boldsymbol{e}}(t)$ as

$$\dot{\tilde{\boldsymbol{e}}}(t) = \sum_{i=1}^{8} h_i \left(\tilde{\boldsymbol{A}}_i\tilde{\boldsymbol{e}}(t) + \tilde{\boldsymbol{S}}_{1i}\tilde{\boldsymbol{w}}(t) \right) \tag{39}$$

where $\tilde{\boldsymbol{S}}_{1i} = \begin{bmatrix} 0 & 0 \\ \boldsymbol{B}_{1i} & 0 \\ 0 & \boldsymbol{I} \end{bmatrix}$, $\tilde{\boldsymbol{w}}(t) = \begin{bmatrix} \boldsymbol{w}(t) \\ \dot{f}(t) \end{bmatrix}$.

To facilitate the following-up FTTC design, Theorem 2 is presented as follows:

Theorem 2. The (39) is asymptotically stable and the $\boldsymbol{H}_\infty$ performance index $\|T_{\tilde{e}v}(t)\|_\infty < \gamma$ can be guaranteed under zero initial condition, if there exist symmetrical matrices $\boldsymbol{H}_{1i}$, $\boldsymbol{H}_{2i}$, K_{1i}, $\gamma > 0$, and the positive symmetrical matrices $\boldsymbol{X}_1 > 0$, $\boldsymbol{P}_2 > 0$, and $\boldsymbol{P}_3 = \boldsymbol{I}$ .Therefore, the following convex optimization problem hold:

$$\min_{\boldsymbol{X}_1,\boldsymbol{P}_2,\boldsymbol{K}_{1i},\boldsymbol{H}_{1i},\boldsymbol{H}_{2i}} \quad \gamma$$

$$s.t. \quad \begin{bmatrix} \boldsymbol{\xi}_i & \boldsymbol{P}\tilde{\boldsymbol{S}}_{1i} & \boldsymbol{\Gamma} & -\boldsymbol{Q}_i & -\boldsymbol{W} \\ * & -\gamma\boldsymbol{I} & 0 & 0 & 0 \\ * & * & -\gamma\boldsymbol{I} & 0 & 0 \\ * & * & * & -\boldsymbol{I} & 0 \\ * & * & * & * & -\boldsymbol{I} \end{bmatrix} < 0 \tag{40}$$

Proof: Define the Lyapunov function as

$$\boldsymbol{V}(t) = \tilde{\boldsymbol{e}}^T(t)\boldsymbol{P}\tilde{\boldsymbol{e}}(t) \tag{41}$$

By taking the derivation along time variable t, we can obtain

$$\dot{V}(t) = \sum_{i=1}^{8} h_i(\tilde{\boldsymbol{e}}^{\mathrm{T}}(t)\left(\tilde{\boldsymbol{A}}^T\boldsymbol{P} + \boldsymbol{P}\tilde{\boldsymbol{A}}\right)\tilde{\boldsymbol{e}}(t) + \tilde{\boldsymbol{w}}^{\mathrm{T}}(t)\tilde{\boldsymbol{S}}_{1i}^{\mathrm{T}}\boldsymbol{P}\tilde{\boldsymbol{e}}(t) + \tilde{\boldsymbol{e}}^{\mathrm{T}}(t)\boldsymbol{P}\tilde{\boldsymbol{S}}_{1i}\tilde{\boldsymbol{w}}(t)) \tag{42}$$

Considering $\tilde{\boldsymbol{w}}(t)$ as the disturbance input and define the $\boldsymbol{H}_\infty$ performance index $\|T_{\tilde{e}\tilde{w}}(t)\|_\infty < \gamma$, that is

$$\|T_{\tilde{e}\tilde{w}}(t)\|_\infty = \frac{\|\tilde{\boldsymbol{e}}(t)\|_2}{\|\tilde{\boldsymbol{w}}(t)\|_2} < \gamma \tag{43}$$

It is easily to transform (43) into

$$\int_0^t (\frac{1}{\gamma}\tilde{\boldsymbol{e}}^T(t)\tilde{\boldsymbol{e}}(t) - \gamma\tilde{\boldsymbol{w}}(t)^T\tilde{\boldsymbol{w}}(t))dt < 0 \tag{44}$$

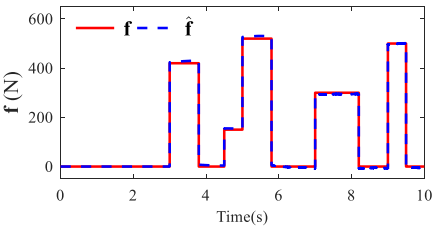

FIGURE 6. The actuator abrupt fault and its estimation via PIO.

To guarantee that system (39) is asymptotically stable, i.e., $\dot{V}(t) < 0$, and synthesizing (42) and (44) yields

$$\int_0^t \left(\begin{bmatrix} \tilde{\boldsymbol{e}}(t) \\ \tilde{\boldsymbol{w}}(t) \end{bmatrix}^T \times \begin{bmatrix} \tilde{\boldsymbol{A}}_i^T\boldsymbol{P} + \boldsymbol{P}\tilde{\boldsymbol{A}}_i + \frac{1}{\gamma}\boldsymbol{I} & \boldsymbol{P}\tilde{\boldsymbol{S}}_{1i} \\ * & -\gamma\boldsymbol{I} \end{bmatrix} \times \begin{bmatrix} \tilde{\boldsymbol{e}}(t) \\ \tilde{\boldsymbol{w}}(t) \end{bmatrix} \right) dt < 0 \tag{45}$$

By taking the same steps from (31) to (38), Theorem 2 is completely proved.

IV. SIMULATION INVESTIGATIONS

Herein, the proposed FTTC scheme is applied to a class of half-vehicle ASS with different types of actuator faults under random and bump road disturbances. The dynamics model of this ASS is shown in Fig. 1 and the parameter values of this model are listed in TABLE 1.

To describe the parametric uncertainties of the ASS, assume that the ranges of m_s, m_{uf} and m_{ur} are [1115, 1355], [48.51, 49.49] and [48.51, 49.49], respectively. Then, the solutions of the above-mentioned LMIs in Theorem 1 and Theorem 2 can be obtained by using LMI tool in MATLAB software, and the gain matrices of PIO and FTTC under the abrupt and time-varying faults can be calculated.

$$\begin{bmatrix} \boldsymbol{A}_i\boldsymbol{X}_1 + \boldsymbol{X}_1\boldsymbol{A}_i^T - \boldsymbol{B}_i\boldsymbol{K}_{1i}\boldsymbol{X}_1 - \boldsymbol{X}_1\boldsymbol{K}_{1i}^T\boldsymbol{B}_i^T & -\boldsymbol{B}_i\boldsymbol{K}_{1i} & -\boldsymbol{B}_i & 0 & \boldsymbol{X}_1 & 0 & 0 \\ * & \boldsymbol{\Omega}_i & \boldsymbol{\Delta}_i & \boldsymbol{P}_2\boldsymbol{B}_{1i} & 0 & \boldsymbol{I} & 0 \\ * & * & \boldsymbol{\chi}_i & 0 & 0 & 0 & \boldsymbol{I} \\ * & * & * & -\gamma\boldsymbol{I} & 0 & 0 & 0 \\ * & * & * & * & -\gamma\boldsymbol{I} & 0 & 0 \\ * & * & * & * & * & -\gamma\boldsymbol{I} & 0 \\ * & * & * & * & * & * & -\gamma\boldsymbol{I} \end{bmatrix} < 0 \tag{35}$$

$$\begin{bmatrix} \boldsymbol{A}_i\boldsymbol{X}_1 + \boldsymbol{X}_1\boldsymbol{A}_i^T & -\boldsymbol{B}_i\boldsymbol{K}_{1i} & -\boldsymbol{B}_i & 0 & \boldsymbol{X}_1 & 0 & 0 \\ * & \boldsymbol{\Omega}_i & \boldsymbol{\Delta}_i & \boldsymbol{P}_2\boldsymbol{B}_{1i} & 0 & \boldsymbol{I} & 0 \\ * & * & \boldsymbol{\chi}_i & 0 & 0 & 0 & \boldsymbol{I} \\ * & * & * & -\gamma\boldsymbol{I} & 0 & 0 & 0 \\ * & * & * & * & -\gamma\boldsymbol{I} & 0 & 0 \\ * & * & * & * & * & -\gamma\boldsymbol{I} & 0 \\ * & * & * & * & * & * & -\gamma\boldsymbol{I} \end{bmatrix} - \begin{bmatrix} \boldsymbol{B}_i\boldsymbol{K}_{1i}\boldsymbol{X}_1 + \boldsymbol{X}_1\boldsymbol{K}_{1i}^T\boldsymbol{B}_i^T & 0 & 0 & 0 & 0 & 0 & 0 \\ 0 & 0 & 0 & 0 & 0 & 0 & 0 \\ 0 & 0 & 0 & 0 & 0 & 0 & 0 \\ 0 & 0 & 0 & 0 & 0 & 0 & 0 \\ 0 & 0 & 0 & 0 & 0 & 0 & 0 \\ 0 & 0 & 0 & 0 & 0 & 0 & 0 \\ 0 & 0 & 0 & 0 & 0 & 0 & 0 \end{bmatrix} < 0 \tag{36}$$

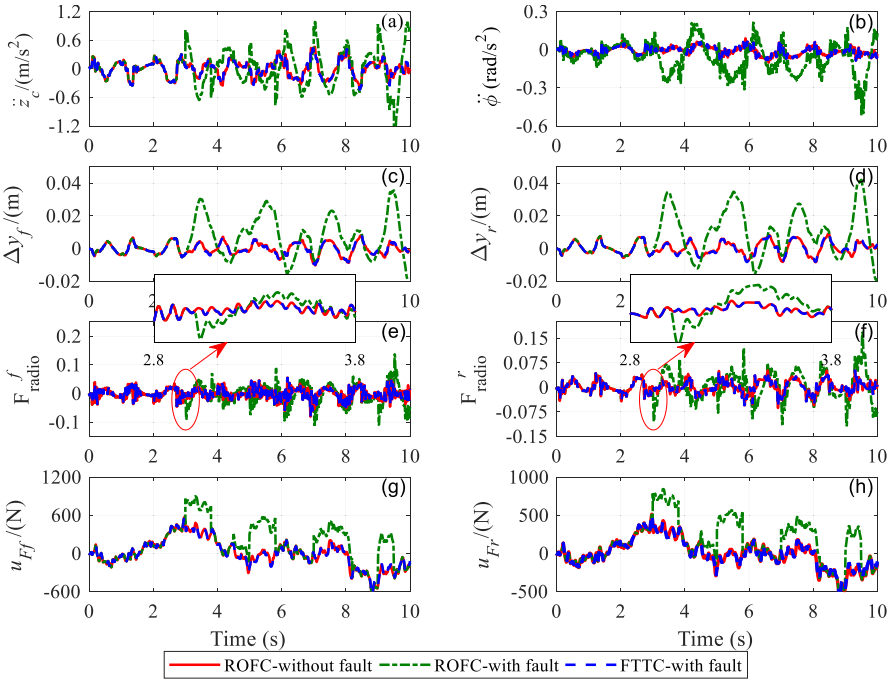

FIGURE 7. The response comparisons of the ASS with the abrupt fault under random road disturbance.

Besides, the weighing coefficients of the ROFC is selected [32] as:

$$\begin{aligned} \boldsymbol{S}_w &= diag\,(0.00014, 0.00014)\,, \\ \boldsymbol{W}_z &= diag\,(W_1, W_2, 1, 1, 1, 1)\,, \\ \boldsymbol{S}_z &= diag\,(6, 3, 20, 20, 0.015, 0.015)\,. \end{aligned}$$

wherein W_1 and W_2 are the corresponding weight function extracted form [37], and their calculation expressions are given by

$$W_1 = \frac{s^2 + 314.2s + 987}{s^2 + 43.98s + 987},$$
$$W_1 = \frac{s^2 + 50.27s + 25.72}{s^2 + 7.037s + 25.72},$$

To analyze the control performance of the designed FTTC, the following three types of vehicle adaptive systems are compared and simulated, as listed below:

- Robust $\boldsymbol{H}_\infty$ output feedback controller under the fault-free condition, denoted as ROFC-without fault;
- Robust $\boldsymbol{H}_\infty$ output feedback controller under the fault condition, denoted as ROFC-with fault;
- Proposed fault-tolerant tracking controller under the fault condition, denoted as FTTC-with fault.

A. PERFORMANCE ANALYSIS OF ASS UNDER ABRUPT FAULT

To verify the availability of the designed FTTC for the ASS with actuator abrupt fault, the random road disturbance described by a Gaussian white noise [38], is employed as the disturbance input to conduct the simulations, which is

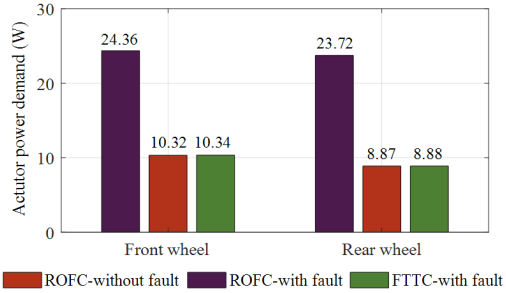

FIGURE 8. The comparisons of power consumption for the ASS in case of ROFC with and without fault, FTTC with fault.

given by

$$G_q\,(n) = G_q\,(n_0)\left(\frac{n}{n_0}\right)^{-c} \tag{46}$$

where $n_0 = 0.1(1/m)$, $c = 2$, and n is the spatial frequency that is determined by the vehicle forward speed V_1 and time-domain frequency f_0 satisfying $f_0 = nV_1$. In the circumstances, we choose B-class highway with $G_q(n_0) = 64 \times 10^{-6}\ \mathrm{m}^3$, and $V_1 = 72(km/h)$.

In addition, consider the following abrupt fault with the defined amplitudes as [35]:

$$\boldsymbol{f}\,(t) = \begin{cases} 420, & 3 < t \le 3.8 \\ 150, & 4.5 < t \le 5 \\ 520, & 5 < t \le 5.8 \\ 300, & 7 < t \le 8.2 \\ 500, & 9 < t \le 9.5 \\ 0, & \text{otherwise} \end{cases} \tag{47}$$

TABLE 2. Comparison of RMS values for ASS performance indicators under actuator abrupt fault.

Symbol	ROFC-without fault	ROFC-with fault	FTTC-with fault
$\ddot{z}_c(\mathrm{m/s^2})$	0.1708	0.3622	0.1729
$\ddot{\phi}(\mathrm{rad/s^2})$	0.03309	0.1304	0.03342
$\Delta y_f(m)$	0.003532	0.01262	0.003539
$\Delta y_r(m)$	0.003886	0.01499	0.003921
F^f_{ratio}	0.0002561	0.0004445	0.0002581
F^r_{ratio}	0.000362	0.0007435	0.0003656
$u_{Ff}(N)$	105.849	245.2	105.4
$u_{Fr}(N)$	100.675	245.4	100.52

what calls for attention is that the abrupt fault in the actuator is introduced when $t = 3s$, which is revealed in Fig. 6 as presenting a zigzag appearance. Obviously, the designed PIO can estimate actuator failures with relative accuracy.

Besides, we use (47) to generate the random road disturbance signal to perform the simulations under non-zero initial condition. Fig. 7 reveals the response comparisons of vehicle suspension performances and the control compensation forces for the three types of ASS (i.e., ROFC-without fault, ROFC-with fault, and FTTC-with fault).

By analyzing each subplot of Fig. 7, one can obtain that, when the ASS runs normally from $0 \sim 3$s, i.e., u_f is zero, which means no extra control is necessary. That is say that the controlled ASS works in case of ROFC-without fault, see the solid red line in Fig. 7. When the fault signal is introduced from 3s to 9.5s, there is an obvious deterioration in $\ddot{z}_c$, $\ddot{\phi}$, Δy_f, Δy_r, F^f_{ratio}, F^r_{ratio}, u_{Ff} and u_{Fr} for the ASS in case of ROFC-with failure, see the green dashed line in Fig. 7. Nevertheless, when the proposed FTTC is applied into the faulty ASS, it is clear that the output responses of the control plant are very consistent with those of the ASS in case of ROFC-without fault, which illustrates that the proposed FTTC can well make up for the performance losses due to the actuator faults, see the blue dashed lines in Fig. 7. Moreover, it is seen from Fig. 7(g) and 5(h) that, the compensation control forces of the FR actuators denoted by u_{Ff} and u_{Fr}, have great changes under ROFC-with fault since it cannot generate the extra control forces for the faulty ASS. However, the proposed FTTC can provide the desired compensation control forces to remove the adverse effects brought about by the actuator abrupt fault.

Additionally, by observing Fig. 7 on the whole, it is easy to see that all the control objectives are guaranteed with the minimization of $|\ddot{z}_c(t)|$ and $\ddot{\phi}(t)$, $F^f_{\mathrm{ratio}} < 1$, $F^r_{\mathrm{ratio}} < 1$, $u_{Ff} < u_{Ff\_\max}$, and $u_{Fr} < u_{Fr\_\max}$, and the similar responses between fault and without fault.

Meanwhile, for the sake of obtaining the power dissipation for these different three types of vehicle ASS, the power demand of each actuator is calculated in terms of the root-mean-square (RMS) according to u_f and $\dot{z}_{sf} - \dot{z}_{uf}$ (or $\dot{z}_{sr} - \dot{z}_{ur}$)

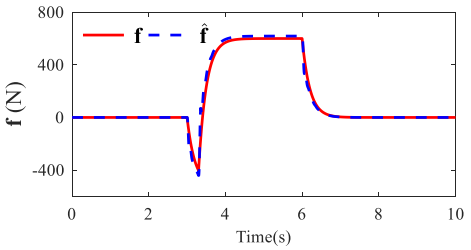

FIGURE 9. The actuator time-varying fault and its estimation via PIO.

at sample time t_i, which is given by [39]

$$P_{\mathrm{RMS}} = \sqrt{\frac{1}{n}\sum_{i=1}^{n}(P(t_i))^2} \tag{48}$$

where

$$P(t_i) = \begin{cases} u_f(t_i)\left(\dot{z}_s(t_i) - \dot{z}_u(t_i)\right), \\ \qquad u_f(t_i)\left(\dot{z}_s(t_i) - \dot{z}_u(t_i)\right) > 0 \\ 0, \qquad\qquad\qquad \text{otherwise} \end{cases} \tag{49}$$

Fig. 8 presents the power consumption for those three types of vehicle ASS. We can draw the conclusion that, compared to the ROFC-without fault, the designed FTTC-with fault had almost the similar control effects and power demands with each other. Yet, for the ROFC-with fault, it has less than desirable control performances, and more specifically, the power consumption of this case is nearly two times of the ROFC-without fault. In contrast, our developed FTTC-with fault shows an obvious advantage in aspects of vehicle suspension performances and power demands.

The comparison of RMS values for the performance indicators of the ASS under actuator abrupt fault are shown in TABLE 2. It is easily seen that the RMS values of the performance indicators for the fault suspension system with the robust output feedback control scheme increases significantly, indicating that the performance of the suspension system deteriorates. The RMS values of performance indicators for the fault suspension system with the proposed control method has little difference with the ones of fault-free suspension system with the robust output feedback control scheme,

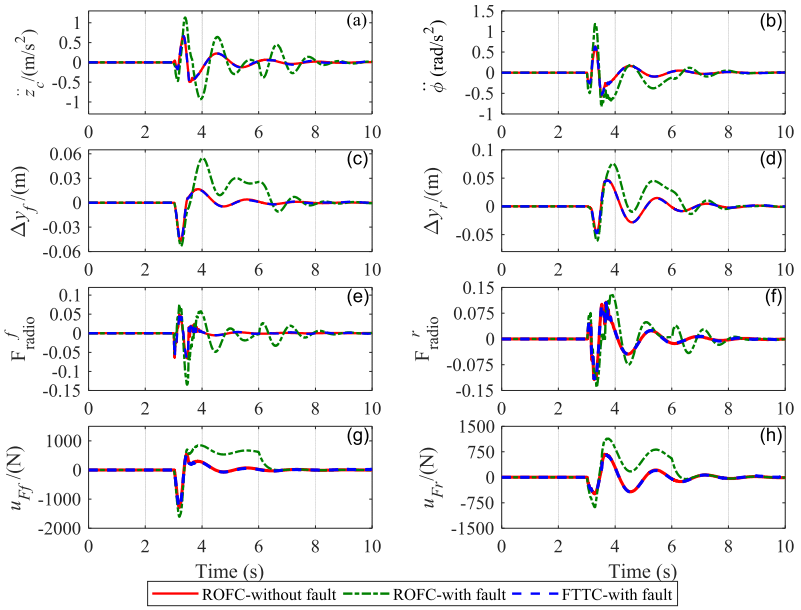

FIGURE 10. The response comparisons of the ASS with the time-varying fault under bump road disturbance.

TABLE 3. Comparison of RMS values for ASS performance indicators under actuator time-varying fault.

Symbol	ROFC-without fault	ROFC-with fault	FTTC-with fault
$\ddot{z}_c(\mathrm{m/s^2})$	0.1486	0.295	0.1483
$\ddot{\phi}(\mathrm{rad/s^2})$	0.1236	0.2481	0.1233
$\Delta y_f(m)$	0.007349	0.01643	0.007317
$\Delta y_r(m)$	0.01311	0.02215	0.01304
F^f_{ratio}	0.0001355	0.0003349	0.0001359
F^r_{ratio}	0.000462	0.0006669	0.0004604
$u_{Ff}(N)$	185.2	389.3	184.8
$u_{Fr}(N)$	178.2	371.9	177.7

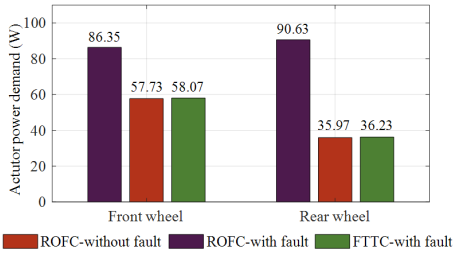

FIGURE 11. The comparisons of power consumption for the ASS in case of ROFC with and without fault, FTTC with fault.

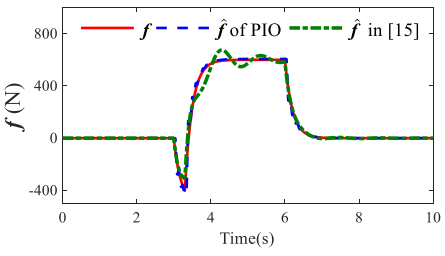

FIGURE 12. The time-varying actuator fault and its estimation using the proposed FTTC and the FTTC in [17] .

which indicates that the proposed fault-tolerant tracking controller can stabilize the performance of suspension system effectively.

B. PERFORMANCE ANALYSIS OF ASS UNDER TIME-VARYING FAULT

To verify the control performances of the recommended FTTC, we use the bump road surface that is extracted from [22] to perform the simulation investigations, and the mathematical expression of this concave convex path is given by

$$z_r(t) = \begin{cases} \frac{A}{2}[1 - cos(2\pi \frac{V}{L}t)], & 3 \le t \le 3 + \frac{V_2}{L} \\ 0, & \text{otherwise} \end{cases} \quad (50)$$

where A, L and V_2 represent the height and length of the bump, and the forward speed of vehicle, respectively, and

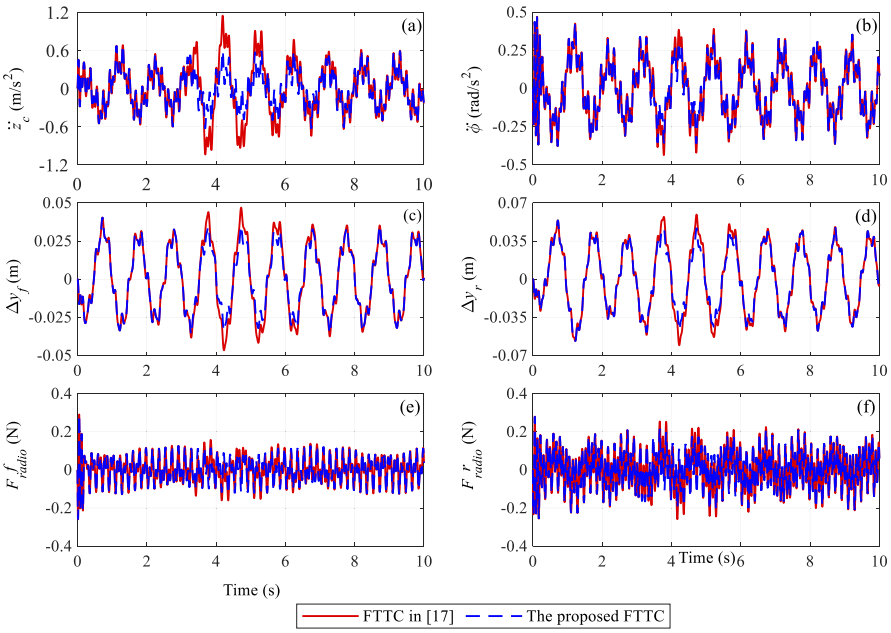

FIGURE 13. The response comparisons of the ASS with the proposed FTTC and the FTTC in [17] in case of the time-varying actuator fault under rough road disturbance.

their corresponding values can be obtained from literatures [28] as $A = 50(mm)$, $L = 5(m)$ and $V_2 = 36(km/h)$.

Moreover, consider the following time-varying fault [36]:

$$\boldsymbol{f}(t) = \begin{cases} -520\left(1 - e^{-5(t-3)}\right), & 3 < t \leq 3.3 \\ -400 + 1000\left(1 - e^{-5(t-3.3)}\right), & 3.3 < t \leq 6 \\ 600e^{-5(t-6)}, & 6 < t \leq 10 \\ 0, & \text{otherwise} \end{cases} \tag{51}$$

It can be seen from (52) that actuator failure is introduced when $t > 3$s, and the time-varying fault signal is shown in Fig. 9, in which the plots display the time-varying actuator failure and its estimation that obtained from the designed PIO. It should be noticed that, during $0 \sim 3$s, the external road disturbance is $z_r = 0$, to reflect the real application scenario, the simulations should be accordingly made under zero initial condition by employing (51).

It is observed from Fig. 9 that the PIO we designed can correctly evaluate the actuator fault produced by (52), and both show good accord with each other. In the following, Fig. 10 shows the response comparisons of vehicle suspension performances and the control compensation forces for the three types of the ASS under bump road disturbance.

It is easily obtained from the subplots of Fig. 10(a) to (f) that, all the performance indicators of this ASS could reach a relative stability state when running under fault-free condition before $t < 3$s. However, when the fault is introduced after $t > 3$s, all of these performance responses have a smoother tendency compared with the other two types of ASS. Overall, the developed FTTC can reduce the vibrations of vehicle body in a shorter time, which can further reduce the negative effects caused by $\boldsymbol{f}(t)$. Similarly, it is observed from Fig. 10 (g) and 8(h) that, when $\boldsymbol{f}(t)$ occurs after $t > 3$s, the desirable control compensation force is accordingly generated by the designed FTTC, which is equivalent to the corresponding control force in case of ROFC-without fault, and this further demonstrates that the negative effective imposed by $\boldsymbol{f}(t)$ can be inhibited. Also, As can be seen from Fig. 10, the minimization of $|\ddot{z}_c(t)|$ and $\ddot{\phi}(t)$ can be pledged, and with the proposed FTTC, the control performances of the faulty ASS can be kept as the same as the corresponding ones of the ASS with the ROFC, Moreover, the other performance requirements are satisfied with $F^f_{\text{ratio}} < 1$, $F^r_{\text{ratio}} < 1$, $u_{Ff} < u_{Ff\_max}$, $u_{Fr} < u_{Fr\_max}$.

The power demand for those three types of vehicle ASS under bump road disturbance is provided in Fig. 11 and based on the histogram plots, when occurring the actuator faults, the proposed FTTC scheme only needs the same power demand as the nominal ROFC method for the controlled uncertain ASS.

Similarly, the comparison of RMS values for the performance indicators of the ASS under actuator abrupt fault are shown in TABLE 3. It is easily seen that the RMS values of the performance indicators for the fault suspension system with the robust output feedback control scheme have great improvement, which implies that the ASS deteriorates to some extent. The RMS values of performance indicators for the fault suspension system with the proposed control method has little difference compared with the ones of fault-free suspension system with the robust output feedback

control scheme, which indicates that the proposed fault-tolerant tracking controller can stabilize the performance of suspension system effectively.

C. COMPARATIVE SIMULATIONS

In this section, the comparative simulations are performed for the robust FTTC in [17] and the proposed FTTC in case of the same actuator fault, and the rough road surface, which is depicted in [33] and given by

$$z_r(t) = 0.0254\sin 2\pi t + 0.005\sin 10.5\pi t + 0.001\sin 21.5\pi t \quad (52)$$

It is noted that the authors [17] adopted a descriptor observer to evaluate the fault information and further to construct the corresponding FTTC, while in our FTTC scheme, the PIO is used to evaluate the different types of actuator faults. Fig. 12 displays the comparisons of the actual time-varying actuator fault of (52) and its estimation using our proposed FTTC and the robust FTTC in [17]. From Fig. 10, the robust FTTC method has a fluctuation error in estimating the fault within 3s $\sim$ 6s, while our proposed FTTC scheme has a relatively higher estimation accuracy for the same fault throughout the simulation time, which demonstrates that our designed PIO can effectively and accurately detect, identify and estimate the actuator fault.

The response comparisons of vehicle suspension performances and the control forces for the proposed FTTC and the FTTC in [17] under rough road disturbance are provided in Fig. 13. The simulation experiment is carried out under non-zero initial condition. Besides, it can be found that, under the rough road surface, the robust FTTC in [17] has the similar control performances at the later simulation stage compared with the proposed FTTC, nevertheless, since the fault are not accurately estimated by the FTTC in [17], the negative effects are scarcely reduced at the beginning of introducing the actuator faults. On the contrary, our proposed FTTC can not only reduce $\ddot{z}_c$ and $\ddot{\phi}$, but also guarantee the suspension hard constraints regardless of the time-varying actuator fault and the rough road disturbance.

V. CONCLUSION AND FUTURE WORKS

This study presents a PIO-based FTTC design method for the ASS subjected to the parameter uncertainty and actuator fault in different road disturbance contexts. First, the parameter uncertainty of the half ASS model is simulated by T-S fuzzy method, and a nominal ROFC is designed to achieve better control performances for the ASS under fault-free mode, whose output responses are taken as the ideal reference trajectories. Next, a composite FTTC scheme consisting of the designed PIO and ROFC is developed to make up for the performance losses due to the actuator faults, and further to render the vehicle suspension to move along the desired reference trajectories. Finally, a case is given to illustrate the availability of the recommended FTTC. In the next work, the actuator and/or sensor fault, the actuator input delays and hard constraints will be considered in the fault-tolerant controller design of the uncertain ASS. It is important to point out that, due to the strong relationship between the performance index of the control object and the reference trajectory, how to choose the suitable reference trajectories needs a further deep study.

APPENDIX A

$$\boldsymbol{A} = \begin{bmatrix} 0 & 1 & 0 & 0 & 0 & 0 & 0 & 0 \\ a_{21} & a_{22} & a_{23} & a_{24} & a_{25} & a_{26} & a_{27} & a_{28} \\ 0 & 0 & 0 & 1 & 0 & 0 & 0 & 0 \\ a_{41} & a_{42} & a_{43} & a_{44} & a_{45} & a_{46} & a_{47} & a_{48} \\ 0 & 0 & 0 & 0 & 0 & 0 & 1 & 0 \\ 0 & 0 & 0 & 0 & 0 & 0 & 0 & 1 \\ a_{71} & a_{72} & a_{73} & a_{74} & a_{75} & 0 & a_{77} & 0 \\ a_{81} & a_{82} & a_{83} & a_{84} & 0 & a_{86} & 0 & a_{88} \end{bmatrix},$$

$$\boldsymbol{B} = \begin{bmatrix} 0 & 0 \\ \frac{1}{m_s} & \frac{1}{m_s} \\ 0 & 0 \\ \frac{-a}{I_y} & \frac{b}{I_y} \\ 0 & 0 \\ 0 & 0 \\ \frac{-1}{m_{uf}} & 0 \\ 0 & \frac{-1}{m_{ur}} \end{bmatrix}, \quad \boldsymbol{B}_1 = \begin{bmatrix} 0 & 0 \\ 0 & 0 \\ 0 & 0 \\ 0 & 0 \\ 0 & 0 \\ 0 & 0 \\ \frac{k_{tf}}{m_{uf}} & 0 \\ 0 & \frac{k_{tr}}{m_{ur}} \end{bmatrix},$$

$$\boldsymbol{C} = \begin{bmatrix} 0 & 1 & 0 & 0 & 0 & 0 & 0 & 0 \\ 0 & 0 & 0 & 1 & 0 & 0 & 0 & 0 \end{bmatrix}, \quad \boldsymbol{D} = [0],$$

$$\boldsymbol{C}_1 = \begin{bmatrix} a_{21} & a_{22} & a_{23} & a_{24} & a_{25} & a_{26} & a_{27} & a_{28} \\ a_{41} & a_{42} & a_{43} & a_{44} & a_{45} & a_{46} & a_{47} & a_{48} \\ 1 & 0 & -a & 0 & -1 & 0 & 0 & 0 \\ 1 & 0 & b & 0 & 0 & -1 & 0 & 0 \\ 0 & 0 & 0 & 0 & k_{tf} & 0 & 0 & 0 \\ 0 & 0 & 0 & 0 & 0 & k_{tr} & 0 & 0 \\ 0 & 0 & 0 & 0 & 0 & 0 & 0 & 0 \\ 0 & 0 & 0 & 0 & 0 & 0 & 0 & 0 \end{bmatrix},$$

$$\boldsymbol{D}_1 = \begin{bmatrix} \frac{1}{m_s} & \frac{1}{m_s} \\ \frac{-a}{I_y} & \frac{b}{I_y} \\ 0 & 0 \\ 0 & 0 \\ 0 & 0 \\ 0 & 0 \\ 1 & 0 \\ 0 & 1 \end{bmatrix}, \quad \boldsymbol{E}_1 = \begin{bmatrix} 0 & 0 \\ 0 & 0 \\ 0 & 0 \\ 0 & 0 \\ -k_{tf} & 0 \\ 0 & -k_{tr} \\ 0 & 0 \\ 0 & 0 \end{bmatrix}.$$

wherein matrix $\boldsymbol{D}$ is a zero matrix with appropriate dimension, and the size of matrix $\boldsymbol{D}$ is dependent on matrix $\boldsymbol{A}$, $\boldsymbol{B}$, $\boldsymbol{B_1}$, $\boldsymbol{C}$; and the corresponding elements in $\boldsymbol{A}$ and $\boldsymbol{C_1}$ are listed as follows:

$$a_{21} = \frac{-k_f - k_r}{m_s}, \quad a_{22} = \frac{-c_f - c_r}{m_s}, \quad a_{23} = \frac{ak_f - bk_r}{m_s},$$

$$a_{24} = \frac{ac_f - bc_r}{m_s}, \quad a_{25} = \frac{k_f}{m_s}, \quad a_{26} = \frac{k_r}{m_s},$$
$$a_{27} = \frac{c_f}{m_s}, \quad a_{28} = \frac{c_r}{m_s}. \quad a_{41} = \frac{ak_f - bk_r}{I_y},$$
$$a_{42} = \frac{ac_f - bc_r}{I_y}, \quad a_{43} = \frac{-a^2k_f - b^2k_r}{I_y},$$
$$a_{44} = \frac{-a^2c_f - b^2c_r}{I_y}, \quad a_{45} = \frac{-ak_f}{I_y}, \quad a_{46} = \frac{bk_r}{I_y},$$
$$a_{47} = \frac{-ac_f}{I_y}, \quad a_{48} = \frac{bc_r}{I_y}. \quad a_{71} = \frac{k_f}{m_{uf}}, \quad a_{72} = \frac{c_f}{m_{uf}},$$
$$a_{73} = \frac{-ak_f}{m_{uf}}, \quad a_{74} = \frac{-ac_f}{m_{uf}} \quad a_{75} = \frac{-k_f - k_{tf}}{m_{uf}},$$
$$a_{77} = \frac{-c_f}{m_{uf}}, \quad a_{81} = \frac{k_r}{m_{ur}}, \quad a_{82} = \frac{c_r}{m_{ur}},$$
$$a_{83} = \frac{bk_r}{m_{ur}}, \quad a_{84} = \frac{bc_r}{m_{ur}}, \quad a_{86} = \frac{-k_r - k_{tr}}{m_{ur}}, \quad a_{88} = \frac{-c_r}{m_{ur}}.$$

REFERENCES

[1] B. Liu, M. Saif, and H. Fan, "Adaptive fault tolerant control of a half-car active suspension systems subject to random actuator failures," *IEEE/ASME Trans. Mechatronics*, vol. 21, no. 1, pp. 845–2857, Dec. 2016, doi: 10.1109/tmech.2016.2587159.

[2] U. S. Pusadkar, S. D. Chaudhari, P. D. Shendge, and S. B. Phadke, "Linear disturbance observer based sliding mode control for active suspension systems with non-ideal actuator," *J. Sound Vib.*, vol. 442, pp. 428–444, Mar. 2019, doi: 10.1016/j.jsv.2018.11.003.

[3] V. Mañosa, F. Ikhouane, and J. Rodellar, "Control of uncertain non-linear systems via adaptive backstepping," *J. Sound Vib.*, vol. 280, nos. 3–5, pp. 657–680, Feb. 2005, doi: 10.1016/j.jsv.2003.12.033.

[4] H. Pang, X. Zhang, and Z. Xu, "Adaptive backstepping-based tracking control design for nonlinear active suspension system with parameter uncertainties and safety constraints," *ISA Trans.*, vol. 88, pp. 23–36, May 2019, doi: 10.1016/j.isatra.2018.11.047.

[5] P. Gaspar, I. Szaszi, and J. Bokor, "Design of robust controllers for active vehicle suspension using the mixed μ synthesis," *Vehicle Syst. Dyn.*, vol. 40, no. 4, pp. 193–228, Oct. 2003, doi: 10.1076/vesd.40.2.193.16541.

[6] S. Huang and W. Lin, "Adaptive fuzzy controller with sliding surface for vehicle suspension control," *IEEE Trans. Fuzzy syst*, vol. 11, no. 4, pp. 550–559, Aug. 2003, doi: 10.1109/TFUZZ.2003.814845.

[7] A. S. Cherry and R. P. Jones, "Fuzzy logic control of an automotive suspension system," *IEEE Proc.-Control Theory Appl.*, vol. 142, no. 2, pp. 149–160, 1995, doi: 10.1049/ip-cta:19951736.

[8] İ. Eski and Ş. Yıldırım, "Vibration control of vehicle active suspension system using a new robust neural network control system," *Simul. Model. Pract. Theory*, vol. 17, no. 5, pp. 778–793, May 2009, doi: 10.1016/j.simpat.2009.01.004.

[9] W. Cai, X. H. Liao, and Y. D. Song, "Indirect robust adaptive fault-tolerant control for attitude tracking of spacecraft," *J. Guid., Control, Dyn.*, vol. 31, no. 5, pp. 1456–1463, Sep. 2008, doi: 10.2514/1.31158.

[10] D. Ye and G. Yang, "Adaptive fault-tolerant tracking control against actuator faults with application to flight control," *IEEE Trans. Control Syst. Technol.*, vol. 14, no. 6, pp. 1008–1096, Oct. 2006, doi: 10.1109/tcst.2006.883191.

[11] B. Jiang, Z. Gao, P. Shi, and Y. Xu, "Adaptive fault-tolerant tracking control of near-space vehicle using Takagi–Sugeno fuzzy models," *IEEE Trans. Fuzzy Syst.*, vol. 18, no. 5, pp. 1000–1007, Oct. 2010, doi: 10.1109/TFUZZ.2010.2058808.

[12] S. Aouaouda, T. Bouarar, and O. Bouhali, "Fault tolerant tracking control using unmeasurable premise variables for vehicle dynamics subject to time varying faults," *J. Franklin Inst.*, vol. 351, no. 9, pp. 4514–4537, Sep. 2014, doi: 10.1016/j.jfranklin.2014.05.012.

[13] S. Liu, H. Zhou, X. Luo, and J. Xiao, "Adaptive sliding fault tolerant control for nonlinear uncertain active suspension systems," *J. Franklin Inst.*, vol. 353, no. 1, pp. 180–199, Jan. 2016, doi: 10.1016/j.jfranklin.2015.11.002.

[14] C. Sentouh, Y. Sebsadji, S. Mammar, and S. Glaser, "Road bank angle and faults estimation using unknown input proportional-integral observer," in *Proc. Eur. Control Conf. (ECC)*, Jul. 2007, pp. 5131–5138, doi: 10.23919/ECC.2007.7068907.

[15] H. Pang, Y. Shang, and P. Wang, "Design of a sliding mode observer-based fault tolerant controller for automobile active suspensions with parameter uncertainties and sensor faults," *IEEE Access*, vol. 8, pp. 186963–186975, 2020, doi: 10.1109/ACCESS.2020.3029815.

[16] H. Pan, H. Li, W. Sun, and Z. Wang, "Adaptive fault-tolerant compensation control and its application to nonlinear suspension systems," *IEEE Trans. Syst., Man, Cybern. Syst.*, vol. 50, no. 5, pp. 1766–1776, May 2020, doi: 10.1109/tsmc.2017.2785796.

[17] S. Aouaouda, M. Chadli, M. Boukhnifer, and H. Karimi, "Robust fault tolerant tracking controller design for vehicle dynamics: A descriptor approach," *Mechatronics*, vol. 30, pp. 316–326, Sep. 2015, doi: 10.1016/j.mechatronics.2014.09.011.

[18] Y.-P. Kuo and T. S. S. Li, "GA-based fuzzy PI/PD controller for automotive active suspension system," *IEEE Trans. Ind. Electron.*, vol. 46, no. 6, pp. 1051–1056, Dec. 1999, doi: 10.1109/41.807984.

[19] Y. M. Sam, J. H. S. Osman, and M. R. A. Ghani, "A class of proportional-integral sliding mode control with application to active suspension system," *Syst. Control Lett.*, vol. 51, nos. 3–4, pp. 217–223, Mar. 2004, doi: 10.1016/j.sysconle.2003.08.007.

[20] M.-H. Do, D. Koenig, and D. Theilliol, "Robust H∞ proportional-integral observer for fault diagnosis: Application to vehicle suspension," *IFAC-PapersOnLine*, vol. 51, no. 24, pp. 536–543, 2018, doi: 10.1016/j.ifacol.2018.09.628.

[21] Y. Zhang and L. Liu, "Adaptive fault tolerant control of active suspension systems with time-varying displacement and velocity constraints," *IEEE Access*, vol. 8, pp. 10847–10856, 2020, doi: 10.1109/access.2020.2964722.

[22] Y. Wei, J. Qiu, H.-K. Lam, and L. Wu, "Approaches to T–S fuzzy-affine-model-based reliable output feedback control for nonlinear it stochastic systems," *IEEE Trans. Fuzzy Syst.*, vol. 25, no. 3, pp. 569–583, Jun. 2017, doi: 10.1109/TFUZZ.2016.2566810.

[23] Y. Wu, B. Jiang, and P. Shi, "Incipient fault diagnosis for T–S fuzzy systems with application to high-speed railway traction devices," *IET Control Theory Appl.*, vol. 10, no. 17, pp. 2286–2297, Nov. 2016, doi: 10.1049/iet-cta.2015.1320.

[24] H. Li, J. Yu, C. Hilton, and H. Liu, "Adaptive sliding-mode control for nonlinear active suspension vehicle systems using T–S fuzzy approach," *IEEE Trans. Ind. Electron.*, vol. 60, no. 8, pp. 3328–3338, Aug. 2013, doi: 10.1109/tie.2012.2202354.

[25] Z. Zhang and J. Dong, "A novel $\mathcal{H}_\infty$ control for T–S fuzzy systems with membership functions online optimization learning," *IEEE Trans. Fuzzy Syst.*, vol. 30, no. 4, pp. 1129–1138, Apr. 2022, doi: 10.1109/TFUZZ.2021.3053315.

[26] D. Ichalal, B. Marx, J. Ragot, and D. Maquin, "Fault detection, isolation and estimation for Takagi–Sugeno nonlinear systems," *J. Franklin Inst.*, vol. 351, no. 7, pp. 3651–3676, Jul. 2014, doi: 10.1016/j.jfranklin.2013.04.012.

[27] Z. Zhang, H. Li, C. Wu, and Q. Zhou, "Finite frequency fuzzy H_∞ control for uncertain active suspension systems with sensor failure," *IEEE/CAA J. Autom. Sinica*, vol. 5, no. 4, pp. 777–786, Jul. 2018, doi: 10.1109/jas.2018.7511132.

[28] L. Qiao and Y. Yang, "Fault-tolerant control for T–S fuzzy systems with sensor faults: Application to a ship propulsion system," *J. Franklin Inst.*, vol. 355, no. 12, pp. 4854–4872, Aug. 2018, doi: 10.1016/j.jfranklin.2018.05.011.

[29] X. Tang, H. Du, S. Sun, D. Ning, Z. Xing, and W. Li, "Takagi–Sugeno fuzzy control for semi-active vehicle suspension with a magnetorheological damper and experimental validation," *IEEE/ASME Trans. Mechatronics*, vol. 22, no. 1, pp. 291–300, Feb. 2017, doi: 10.1109/tmech.2016.2619361.

[30] H. Pang, F. Liu, and Z. Xu, "Variable universe fuzzy control for vehicle semi-active suspension system with MR damper combining fuzzy neural network and particle swarm optimization," *Neurocomputing*, vol. 306, pp. 130–140, Sep. 2018, doi: 10.1016/j.neucom.2018.04.055.

[31] H. Li, H. Gao, P. Shi, and X. Zhao, "Fault-tolerant control of Markovian jump stochastic systems via the augmented sliding mode observer approach," *Automatica*, vol. 50, no. 7, pp. 1825–1834, Jul. 2014, doi: 10.1016/j.automatica.2014.04.006.

[32] C. Scherer, P. Gahinet, and M. Chilali, "Multi-objective output-feedback control via LMI optimization," *IEEE Trans. Automat.*, vol. 42, no. 7, pp. 896–911, Jul. 1997, doi: 10.1016/s1474-6670(17)57912-4.
[33] H. Li, H. Gao, H. Liu, and M. Liu, "Fault-tolerant H_∞ control for active suspension vehicle systems with actuator faults," *Proc. Inst. Mech. Eng., I, J. Syst. Control Eng.*, vol. 226, no. 3, pp. 348–363, Mar. 2012, doi: 10.1177/0959651811418401.
[34] J. Qiao, D. Zhang, Y. Zhu, and P. Zhang, "Disturbance observer-based finite-time attitude maneuver control for micro satellite under actuator deviation fault," *Aerosp. Sci. Technol.*, vols. 82–83, pp. 262–271, Nov. 2018, doi: 10.1016/j.ast.2018.09.007.
[35] Y. Wu, B. Jiang, and N. Lu, "A descriptor system approach for estimation of incipient faults with application to high-speed railway traction devices," *IEEE Trans. Syst., Man, Cybern. Syst.*, vol. 49, no. 10, pp. 2108–2118, Oct. 2019, doi: 10.1109/TSMC.2017.2757264.
[36] Z. Han, K. Zhang, and H. Liu, "Actuator fault reconstruction based on a robust adaptive observer," *IET Control Theory Appl.*, vol. 12, no. 15, pp. 2076–2087, Oct. 2018, doi: 10.1049/iet-cta.2018.0112.
[37] H. D. Choi, C. K. Ahn, P. Shi, L. Wu, and M. T. Lim, "Dynamic output-feedback dissipative control for T–S fuzzy systems with time-varying input delay and output constraints," *IEEE Trans. Fuzzy Syst.*, vol. 25, no. 3, pp. 511–526, Jun. 2017, doi: 10.1109/TFUZZ.2016.2566800.
[38] J. Wang, D. Wilson, and G. Halikias, "H_∞ robust-performance control of decoupled active suspension systems based on LMI method," in *Proc. ACC*, vol. 4, 2001, pp. 2658–2663, doi: 10.1109/ACC.2001.946278.
[39] G. Feng, "A survey on analysis and design of model-based fuzzy control systems," *IEEE Trans. Fuzzy Syst.*, vol. 14, no. 5, pp. 676–697, Oct. 2006, doi: 10.1109/TFUZZ.2006.883415.

JIBO LUO received the B.S. degree in vehicle engineering from the Xi'an University of Technology, where he is currently pursuing the M.S. degree in mechanical engineering. His research interest includes active suspension fault-tolerant control.

HUI PANG (Member, IEEE) received the B.S. degree in mechanical manufacturing and automation from the Zhengzhou Institute of Aeronautical Industry Management, Zhenzhou, China, in 2002, and the M.S. and Ph.D. degrees in mechanical engineering from Northwestern Polytechnical University, Xi'an, China, in 2005 and 2009, respectively.

From November 2016 to November 2017, he was a Visiting Scholar at the Department of Automotive Engineering, Clemson University, Greenville, SC, USA. He is currently an Associate Professor with the School of Mechanical and Precision Instrument Engineering, Xi'an University of Technology. His interests include nonlinear robust control and fuzzy sliding mode control and their applications in vehicle dynamics control.

MINGXIANG WANG received the B.S. degree in vehicle engineering from the Xi'an University of Technology, where he is currently pursuing the M.S. degree in mechanical engineering. His research interest includes active suspension optimal control.

RUI YAO received the B.S. degree in vehicle engineering from Southwest Petroleum University and received the M.S. degree in mechanical engineering from the Xi'an University of Technology. His research interest includes active suspension lateral control.